



## OPEN Incorporation of seasonal land cover to develop seasonally integrated land cover map for change detection in Dhaka mega City

Md. Sharafat Chowdhury<sup>1,2</sup>✉

The seasonal cycle significantly alters the spatial extent of land cover (LC); and restricts capturing LC dynamics using a single-date satellite image. This study proposes a new method for producing a Seasonally Integrated Land Cover (SILC) by combining seasonal LCs to capture these rotational land covers. Additionally, SILC has been used to detect land cover changes in Dhaka City between 2000 and 2022. Results showed that SILC exchange occurred among every SILC over the study period, though some were negligible. The major drivers of SILC change in Dhaka City (2000–2022) were the significant expansion of built-up areas (77.80 to 143.75 sq km) and the significant reduction of seasonal wetland vegetation (91.12 to 6.62 sq km). Unplanned urban expansion in and around the city center increased the spatial extent of permanent built-up areas by converting seasonal built-up (16.33 sq km), dry-land vegetation (12.26 sq km), bare land (8.87 sq km), wetland vegetation (7.72 sq km) and permanent (8.03 sq km) and mixed (5.12 sq km) vegetation. Additionally, large areas of seasonal wetland (28.29 sq km) and dry-land vegetation (16.17 sq km) were converted into permanent vegetation due to anthropogenic activities, basically landfilling, shifting its distribution to the peripheral areas, especially in the east. This change also decreased seasonal variation in LCs over time. The SILC maps provide critical insights for Dhaka's urban planning, supporting flood mitigation, green space conservation, wetland restoration, and infrastructure planning. Also helps in regulating urban growth, flood mitigation, and enhance climate resilience through targeted land-use policies.

**Keywords** Geographic information systems, Land cover classification, Seasonality, Change detection, Urban sustainability

Land cover (LC) mapping and change detection are crucial in geospatial and remote sensing applications due to their significant role in various scientific research<sup>1</sup> such as environmental monitoring and modeling<sup>2,3</sup>, climate studies<sup>4</sup>, resource management<sup>5</sup>, sustainable urban development, and urban planning<sup>6,7</sup>. Additionally, accurate LC maps and LC change detection provide valuable insights into land use dynamics driven by both natural and anthropogenic processes, often with decision-making and policy implications<sup>8,9</sup>. Globally, land cover (LC) changes driven by rapid urbanization pose serious threats to global cities by increasing health hazards, air pollution, acid rain, urban heat island effects, and urban flooding<sup>10</sup>. Moreover, LC changes are affecting natural biological processes, urban ecology and environment, and natural habitat, ultimately threatening the sustainable development of urban areas<sup>11–14</sup>. In developing countries, urban expansion is discrete which affects the proper implementation of plans and policy, no exception is Dhaka<sup>15</sup>. As a result, the requirement for a more accurate LC is of significant importance.

Land Cover (LC) classification and change detection is widely carried out using Geographic Information Systems (GIS) and remote sensing across the world. Traditional methods rely on single-date imagery, which fails to capture seasonally altered LC classes<sup>16,17</sup>. Because, some land covers (LCs), influenced by both natural and anthropogenic processes, exhibit inter-seasonal changes, especially in tropical areas<sup>18,19</sup>, returning to their

<sup>1</sup>Centre for Remote Sensing and GIScience, Dhaka, Bangladesh. <sup>2</sup>Department of Geography and Environment, Jahangirnagar University, Dhaka 1342, Bangladesh. ✉email: sharafat.44@geography-juniv.edu.bd; sharafat.geography.juniv@gmail.com

original state after completing their phenological cycles<sup>20–22</sup>. For example, in Dhaka, wetlands expand in rainy and post-monsoon seasons and shrink in winter and summer and sometimes in dry seasons used for agriculture. Agricultural lands altered into cultivated (vegetation) in winter and fallow states (bare) in summer, whereas low-lying agricultural lands transformed into wetlands (water bodies) during monsoon (Fig. 1). Moreover, areas covered by built-up, vegetation and bare land also fluctuate according to the seasons over the year<sup>18,19</sup>. The schematic diagram (Fig. 1) shows the seasonal rotational pattern of the LC in Dhaka City during different seasons. Single date LC classification, overlooking seasonal rotations, often leads to overestimation or underestimation of certain classes, which is evident in previous studies of Dhaka City<sup>23–26</sup>. Despite its importance, limited research has addressed these seasonal variations comprehensively, as studies have primarily focused on fixed LC types.

Globally, to reduce the seasonality effect emphasis has been given to pre-classification techniques such as spectral mixing of satellite images<sup>27,28</sup>, selecting the best season for LC mapping for selected land features<sup>17</sup>, comparing the LC maps of different seasons to select the best season<sup>29</sup>, extraction of seasonal features from different season from time series satellite data and superimposing them to get the accurate LC map<sup>30</sup>, selection of image acquisition timing by temporal optimization of image acquisition<sup>16</sup>, spectral-mixing/adding values from annual time series satellite data<sup>31</sup>, eliminating spurious changes in LC change map aroused due to seasonal effect in LC classification<sup>32</sup>, and combining the raw images of different seasons/months<sup>33</sup>. Multi-temporal image

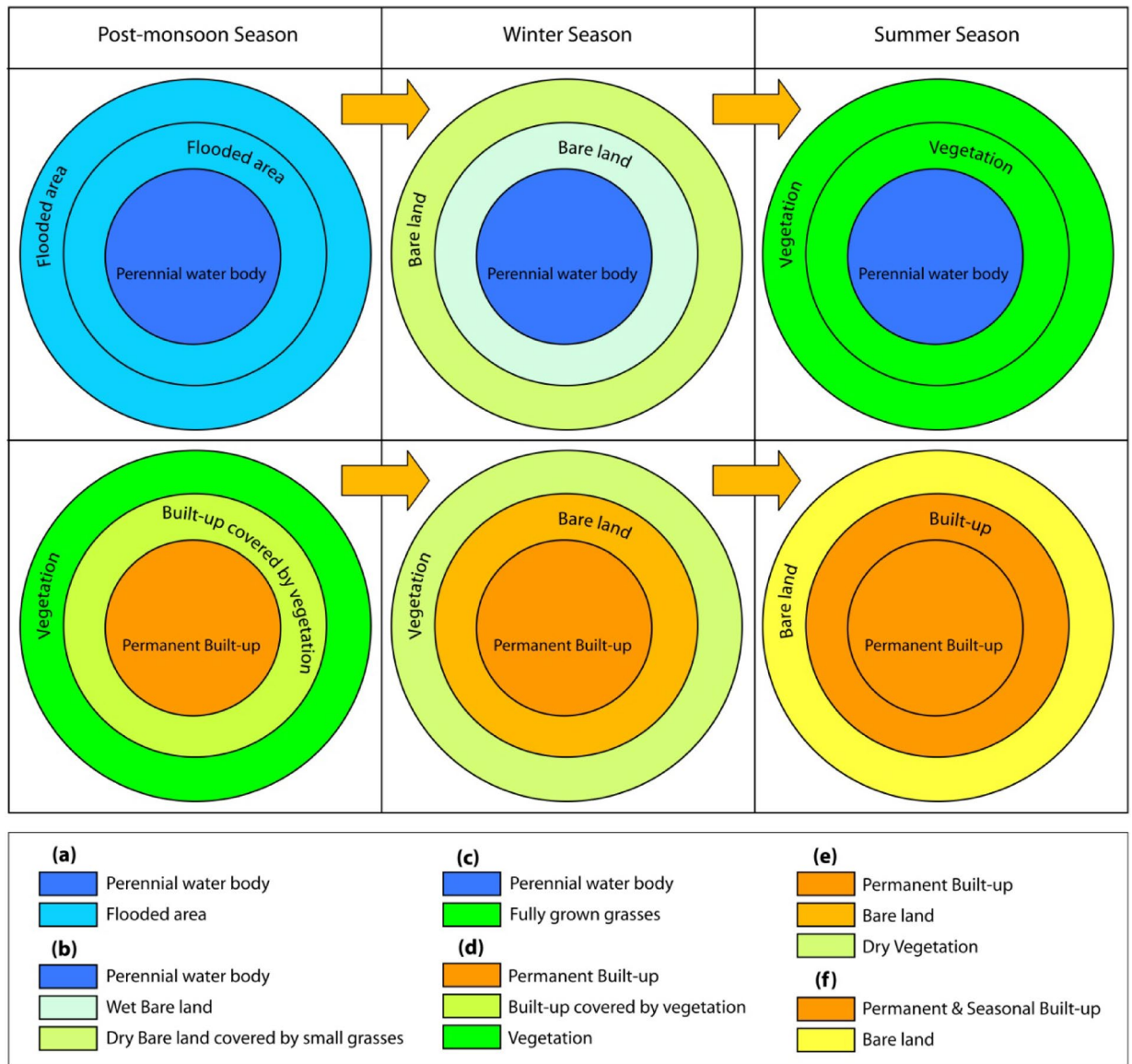


**Fig. 1.** Pattern of seasonal rotational land covers in Dhaka City. Figure a-c shows that some lands become flooded during the pre-monsoon season, become bare during the winter season and are covered by well-grown vegetation during the summer season. Figure d-f shows that some vegetation becomes dry during the winter season and becomes fully bare during the summer season. Additionally, some built-up areas are covered by healthy vegetation during post-monsoon which becomes dry during winter as the vegetation becomes dry and marked as built-up areas in summer as the leaves fall completely from the tree.

classification slightly improves the accuracy of LC maps due to the high similarity in the seasonal changes of the LC classes<sup>33</sup>. But, still now delineating the best-classified image replicating the real landscape remains undeveloped. However, limited effort has been given to seasonally altering LCs across the world as well as in Dhaka.

Previously land cover of Dhaka city was classified into built-up areas, vegetation, bare land, and water bodies<sup>25,34,35</sup> and some researchers added other types of land use and land cover along with these four types such as agricultural land<sup>26,36,37</sup>, agriculture and wetland<sup>38,39</sup>, lowland<sup>24</sup>, dense vegetation and sparse vegetation<sup>25</sup>. However, seasonality significantly affects land cover areas in the classified maps because the same areas may transform into vegetation/agriculture and bare land across seasons. This seasonal variability also affects vegetation in urban parks and playgrounds<sup>19,38</sup>. Due to the higher heterogeneity of land cover in the urban area, it is very difficult to demarcate varieties of LC which affects decision-making, land use policy and environmental degradation assessment which leads to unsustainable development of the city<sup>15,38</sup>. However, in Dhaka, limited effort has been made to address the impact of seasonality in LC classification or to categorize seasonally altered LCs. Most studies focus on classifying LC for individual seasons and analyzing seasonal variations in land cover extent rather than integrating seasonal dynamics into a comprehensive classification approach<sup>18</sup>.

Considering the issues, the current research proposes a conceptually and methodologically novel method to capture seasonally altered LC classes through the development of a Seasonally Integrated Land Cover (SILC) classification system. This study hypothesizes that preparing SILC maps by integrating seasonal LC maps will provide a more accurate and realistic representation of land cover dynamics compared to single-date LC maps, improving urban planning and climate resilience strategies. To prepare SILC maps for Dhaka city, four basic LC types of built-up area, vegetation, bare land, and water body, which are extensively studied and widely accepted<sup>25,34,35</sup>, were used to identify and reclassify the seasonally altered LCs.

A unique rule-based spatial reclassification logic was applied, where seasonal LC classes were combined into eleven final SILC categories (e.g., seasonal wetland vegetation, mixed urban, seasonal dry-land vegetation, permanent water, permanent built-up, permanent vegetation, permanent bare land, seasonal built-up, seasonal bare land) (full definition in Table 5), based on their temporal behaviour, environmental and geographical characteristics and contextual relevance in an urban monsoon climate. The LC maps of three seasons, namely post-monsoon, winter and summer, were integrated for each target year (2000, 2010, and 2022) to prepare SILC maps. Change detection was performed using these SILC maps to understand the spatio-temporal transformation of land cover in Dhaka over a 22-year period. The study prioritized long-term temporal consistency over spatial resolution to capture multidecadal land cover changes in Dhaka, making Landsat the most appropriate data source.

This research goes beyond conventional single-season or spectral-composite approaches by capturing intra-annual land cover dynamics and reclassifying them into temporally stable or seasonally transitional categories. The proposed SILC framework offers a replicable method that can be applied to other seasonally dynamic urban areas, particularly in tropical monsoon regions, for better environmental management, hazard assessment, and land use planning. The specific objectives of the research are:

- To prepare LC for three seasons of post-monsoon, winter and summer of the years 2000, 2010 and 2022.
- To prepare the Seasonally Integrated LC (SILC) by combining the LC of the three seasons of a given year by considering the seasonally rotational LCs.
- To assess the SILC change between 2000 and 2022 in Dhaka City.

Compared to single-date LC maps, this type of SILC map will be more useful for urban planning and policy-making towards a sustainable and climate-resilient city.

## Results

### Inter-seasonal pattern of four basic LCs from 2000 to 2022

The seasonal land cover (LC) analysis from 2000 to 2022 exhibited distinct spatial variations within each year due to seasonal impact, especially in vegetation cover, water bodies and bare land (Fig. 2.a-i). Seasonal changes in land cover (LC) were more evident in the early years (Fig. 2.a, 2.b and 2.c); however, they declined over time due to urban expansion and related development activities (Fig. 2.g, h and i), which permanently converted some seasonally dynamic LCs (Fig. 4.a, 2.b and 2.c). In 2000, a large extent of water bodies on the east and west sides of the city during the post-monsoon season transformed into vegetation cover during the winter and summer seasons (Fig. 2.a, 2.b and 2.c). Additionally, some vegetation cover in the northern part of the city was converted into bare land from winter to summer (Fig. 2.a, 2.b and 2.c). In 2010, most of these seasonal changes occurred in the eastern and the northwestern parts of the city (Fig. 2.d, 2.e and 2.f). In 2022, the magnitude of seasonal fluctuations significantly declined, except for minor changes in the southeastern part of the city (Fig. 2.g, 2.h and 2.i).

This decrease in seasonal transitions in LCs over time was driven by unplanned development activities in areas with seasonally altering LCs. For Example, some seasonal vegetation has been permanently replaced by bare land or built-up areas (Table S 2), reducing seasonal variability in LCs, especially in built-up areas (Table 2 and Table S 2). However, in the later years (2010 and 2022), post-monsoon vegetation cover in core urban areas was altered into impervious surfaces (built-up areas or bare land) during winter and summer (Fig. 2.d to 2.i). This change might be attributed to the excessive urban island effect, which affects the spectral reflectance of vegetation during dry seasons. Though vegetation cover is reduced in the city hub, due to some agricultural activity in the peripheral area of the city, the total area of vegetation cover remains almost unchanged during post-monsoon and summer (Fig. 3 and Table S 1). These seasonal alterations of LC had been overlooked in a single-date LC map but it is now largely evident in the current research. The effect of seasonality is also evident in

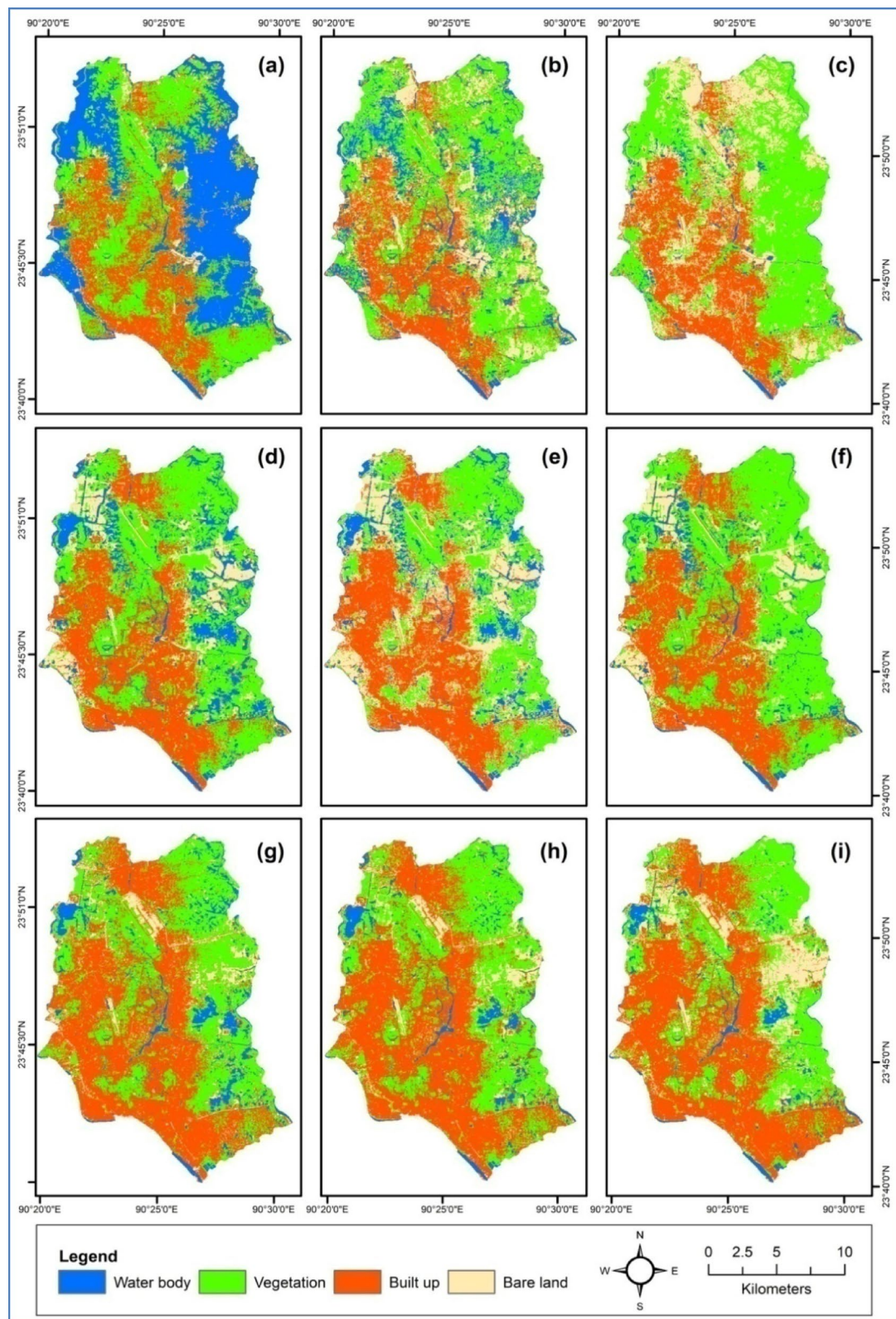


**Fig. 2.** LC of (a) post-monsoon, (b) winter, and (c) summer of the year 2000, (d) post-monsoon, (e) winter, and (f) summer of the year 2010 and (g) post-monsoon, (h) winter, and (i) summer of the year 2022. Maps were generated using QGIS 3.26.1 (QGIS Development Team, <https://qgis.org>) and ArcGIS 10.5 (Esri, <https://www.esri.com>).

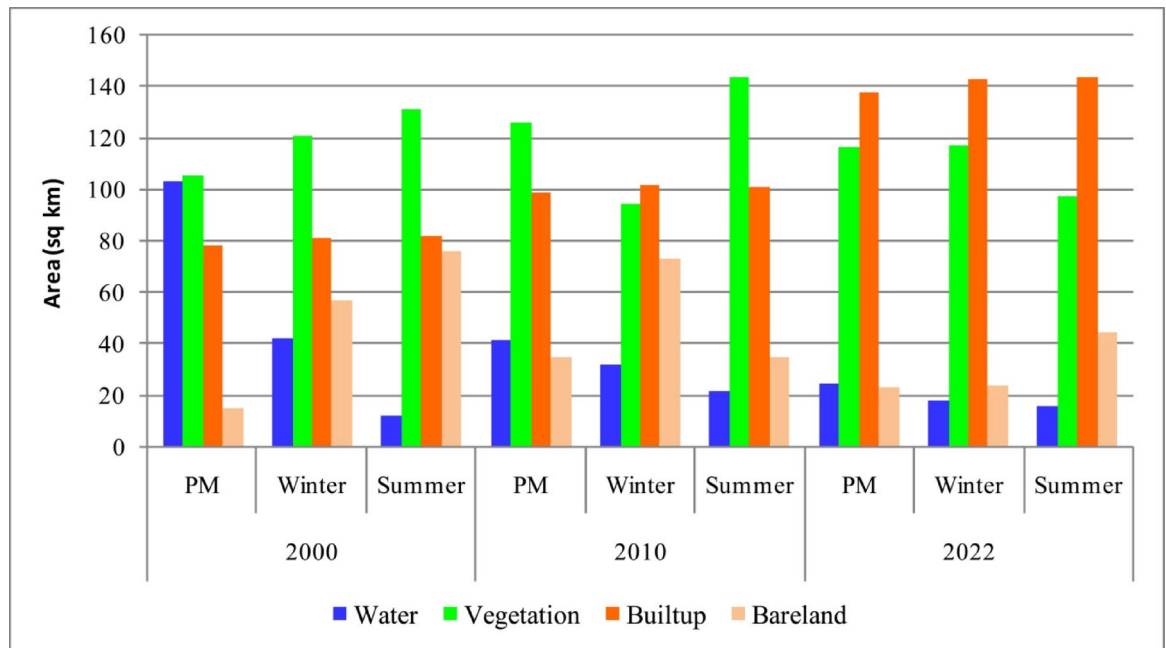


**Fig. 3.** Trend of LC in Dhaka from 2000 to 2022.

the long-term change of the LC classes (Fig. 3). Over time water bodies and vegetation largely decreased whereas built-up areas and bare land significantly increased (Fig. 3).

#### SILC changes from 2000 to 2022

These seasonal fluctuations of the LC classes (Fig. 2.a-i) are engaged to produce the SILC map of a single year (Fig. 4.a-c). From the combination of the three seasons' map, the dynamic SILC map revealed the information on the seasonally fluctuating LC classes. The combined map showed eleven SILC classes in the three studied years (Table 1; Fig. 3 and the definition of SILC in Table 6).

Between the years 2000 and 2022, permanent built up, and permanent vegetation have largely increased and permanent bare land and mixed urban slightly increased (Table 1). On the other hand, seasonal wetland vegetation (Fig. 4.a-c), once which was also been cultivated during the dry seasons, significantly decreased followed by seasonal bare land, mixed vegetation and seasonal dry-land vegetation (Table 1).

The total built-up area expanded from 77.80 sq km in 2000 to 143.75 sq km in 2022 (Table 1), reflecting rapid urbanization and development activity and increased population pressure (Fig. 4). Seasonal vegetation pattern (Fig. 4), which fluctuated significantly in 2000 (Fig. 2.a-c), has become more static in 2022 (Fig. 2.g-i), with a sharp reduction in seasonal wetland vegetation (from 30.28 to 2.20%) and an increase in permanent built-up areas (from 16.92 to 36.88%) (Table 1). This change is driven by the rise in human activity and urban heterogeneity, resulted in the increase of mixed urban, bare land and built-up areas. Such as filled-up areas with sand for housing purposes classified as wetland during post-monsoon, vegetation during winter and built up during summer, slightly increasing seasonal fluctuation in LCs, particularly mixed SILCs. Moreover, a decrease in seasonal built-up and an increase in mixed urban areas indicate the reduction of vegetation cover around and in between urban areas, such as reduction of parks and building-front gardens, which is illustrated in the middle part of the classified images (Fig. 4.a-c). Additionally, rapid urbanization has also resulted in the infilling of large water bodies, especially wetlands, for infrastructure development. The seasonal wetland vegetation decreased from 91.12 sq km in 2000 to just 6.62 sq km in 2022 (Table 1), contributing to a more homogenized land cover composition in recent years. However, government interventions, such as the restoration of Hatirjheel<sup>40</sup> and the conversion of some seasonal water bodies and wetland vegetation in the northern part of the city which is also evident in Ahmed & Ahmed (2012)<sup>41</sup>, have contributed to a slight increase in permanent water bodies in certain areas (Fig. 2.a-i and 4.a-c). The permanent bare land, increased from 7.84 sq km in 2000 to 22.00 sq km in 2010, before decreasing to 13.48 sq km in 2022 (Table 1). Whereas, seasonal bare land followed a decreasing trend, declining from 23.14 sq km in 2000 to 14.06 sq km in 2010 and further to 9.39 sq km in 2022 (Table 1).

#### Seasonal dynamics and urban expansion

The spatial distribution of seasonal LC changes demonstrates the role of urban expansion in modifying natural land cover. In 2000, transformations of seasonal vegetation and wetlands were concentrated on the periphery of Dhaka (Fig. 2.a-c). However, by 2010 and 2022, these changes had transferred towards the urban core areas, driven by the conversion of green spaces into impervious surfaces (Fig. 2.d-i). This inter-seasonal pattern is also reflected in the SILCs, where most of the seasonal SILC such as seasonal built-up, seasonal dry-land vegetations and seasonal bare land largely converted into permanent type SILC such as permanent built-up (Fig. 4.a-c and Fig. 5). This pattern is also evident in the north part of the city (Fig. 4.a-c and Fig. 5). This pattern of SILC change

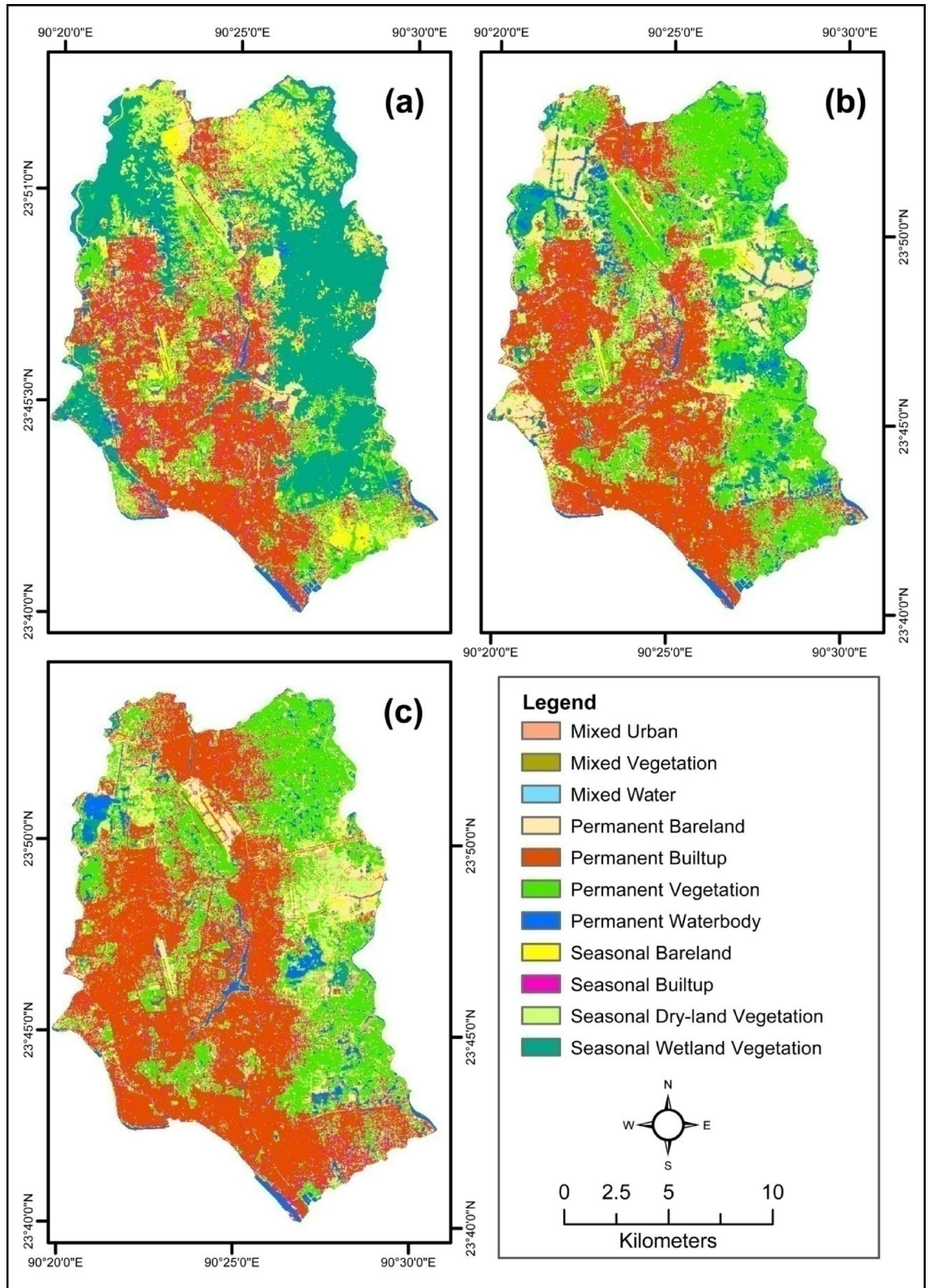


**Fig. 4.** SILC of the year (a) 2000, b) 2010 and (c) 2022. Note: These figures illustrate the actual scenario of LC in a single year by integrating the dynamic LCs that have an inter-seasonal changing nature in Dhaka city. Maps were generated using QGIS 3.26.1 (QGIS Development Team, <https://qgis.org>) and ArcGIS 10.5 (Esri, <https://www.esri.com>).

LULC	Area (Km <sup>2</sup> )			Area (percentage)			Difference (percentage)		
	2000	2010	2022	2000	2010	2022	2000–2010	2010–2022	2000–2022
Permanent Water body	9.32	15.07	12.09	3.10	5.01	4.02	1.91	-0.99	0.92
Seasonal Wetland Vegetation	91.12	24.49	6.62	30.28	8.14	2.20	-22.14	-5.94	-28.08
Mixed Water	0.89	0.13	0.04	0.29	0.04	0.01	-0.25	-0.03	-0.28
Seasonal Bare land	23.14	14.06	9.39	7.69	4.67	3.12	-3.02	-1.55	-4.57
Seasonal Dry-land Vegetation	43.13	37.49	39.00	14.33	12.46	12.96	-1.87	0.50	-1.37
Mixed Vegetation	10.92	5.66	3.26	3.63	1.88	1.08	-1.75	-0.80	-2.55
Permanent Vegetation	33.31	80.26	73.01	11.07	26.67	24.26	15.60	-2.41	13.19
Seasonal Built-up	23.65	18.23	20.94	7.86	6.06	6.96	-1.80	0.90	-0.90
Mixed Urban	6.70	5.36	12.15	2.23	1.78	4.04	-0.44	2.26	1.81
Permanent Built-up	50.93	78.19	110.98	16.92	25.98	36.88	9.06	10.90	19.95
Permanent Bare land	7.84	22.00	13.48	2.61	7.31	4.48	4.71	-2.83	1.87

**Table 1.** SILC change between 2000 and 2022 derived from combined map.

aligns with the rapid population growth and infrastructure development of Dhaka city. During the study time (2000 to 2022), although a minor change was evident in all SILCs, however, significant land exchanges occurred between seasonal vegetation, bare land, and built-up types (Fig. 5a and b and Table S 2–4). For example, between 2000 and 2010, 21.95 km<sup>2</sup> of seasonal wetland vegetation was converted into permanent vegetation, whereas, 13.56 km<sup>2</sup> of seasonal built-up was converted into permanent built-up areas (Table S 2). From 2010 to 2022, this trend continued, with an additional 11.38 km<sup>2</sup> of seasonal built-up converting into permanent built-up areas (Table S 3). These findings indicate a significant increase in permanent urban structures, reducing seasonal land cover variability in Dhaka.

### Drivers of SILC change in Dhaka City

Drivers of SILC change were assessed by employing change detection techniques. Table S 2, 3 and 4 shows the SILC exchange scenarios and their loss and gain according to each feature type of the years 2000–2010, 2010–2022 and 2000–2022, respectively. The SILC change scenario shows that SILC exchange has occurred in almost all the types but some changes are negligible. The conversion of seasonal wetland vegetation and other vegetation and bare land to permanent vegetation was the major driver of SILC change in Dhaka. Drivers of permanent SILC classes are under consideration in this research.

Table S 2 shows that between 2000 and 2010, a significant amount of seasonal wetland vegetation converted into permanent vegetation (21.95 sq km) followed by permanent bare land (15.99), seasonal dry-land vegetation (11.91 sq km) and permanent water body (8.26 sq km). Permanent vegetation largely increased by seasonal dry-land vegetation (22.16 sq km), seasonal wetland vegetation (21.95 sq km), and seasonal bare land (8.84 sq km) and decreased by seasonal dry-land vegetation (5.80 sq km), permanent built-up (2.64 sq km) and seasonal built up (1.55 sq km) (Table S 2). Most of the LC classes significantly contributed to permanent built-ups such as seasonal built-up (13.56 sq km), seasonal dry-land vegetation (4.87 sq km), seasonal bare land (4.83 sq km), mixed vegetation (3.09 sq km), permanent vegetation (2.64 sq km), permanent bare land (1.92), mixed urban (1.75 sq km) and seasonal wetland vegetation (1.74 sq km) (Table S 2).

Table S 3 shows that between 2010 and 2022, a large amount of seasonal wetland vegetation converted into other LC classes and a higher amount converted into permanent vegetation (5.60 sq km) followed by seasonal dry-land vegetation (4.92 sq km) and permanent water body (3.55 sq km). Another significant increment occurred in permanent built-up areas where a significant amount of seasonal built-up (11.38 sq km) converted into permanent built-up followed by permanent vegetation (8.24 sq km), seasonal dry-land vegetation (7.17 sq km), seasonal bare land (4.10 sq km), permanent bare land (3.53 sq km), mixed urban (2.27 sq km), and mixed vegetation (2.09 sq km) (Table S 3). A higher amount of seasonal dry-land vegetation (11.72 sq km) converted into permanent vegetation. Some permanent vegetation converted into seasonal dry-land vegetation (6.04 sq km) and permanent vegetation (4.25 sq km) (Table S 3).

Table S 4 shows that between 2000 and 2022, a significant amount of seasonal wetland vegetation (84.51 sq km) was converted into other LCs and a significant amount of other LC classes (60.05 sq km) was converted into permanent built-up areas. Besides seasonal wetland vegetation (28.29 sq km), the seasonal dry-land vegetation (16.17 sq km) and seasonal bare land (5.52 sq km) largely contributed to the increment of permanent vegetation. On the other hand, a large amount of permanent vegetation was converted into permanent built-up (8.03 sq km), seasonal dry-land vegetation (4.06 sq km) and seasonal built-up (2.75 sq km) (Table S 4). The conversion of permanent vegetation cover shifted its spatial distribution to the peripheral areas of the city, especially on the east side, where seasonal wetland and dry-land vegetation were dominant during 2000 (Figs. 4 and 5). In the last two decades, SILC change largely occurred due to an increment of permanent built-up areas, followed by permanent vegetation, permanent bare land and mixed urban and a decrement of seasonal wetland vegetation, followed by seasonal bare land, mixed vegetation, and seasonal dry-land vegetation. Whereas, major derives are the increase in permanent built-up areas and the decrease in seasonal wetland vegetation (Table S 4). The spatial distribution is largely affected by the alteration of seasonal wetland vegetation to permanent vegetation along with unplanned urban growth (Figs. 4 and 5).

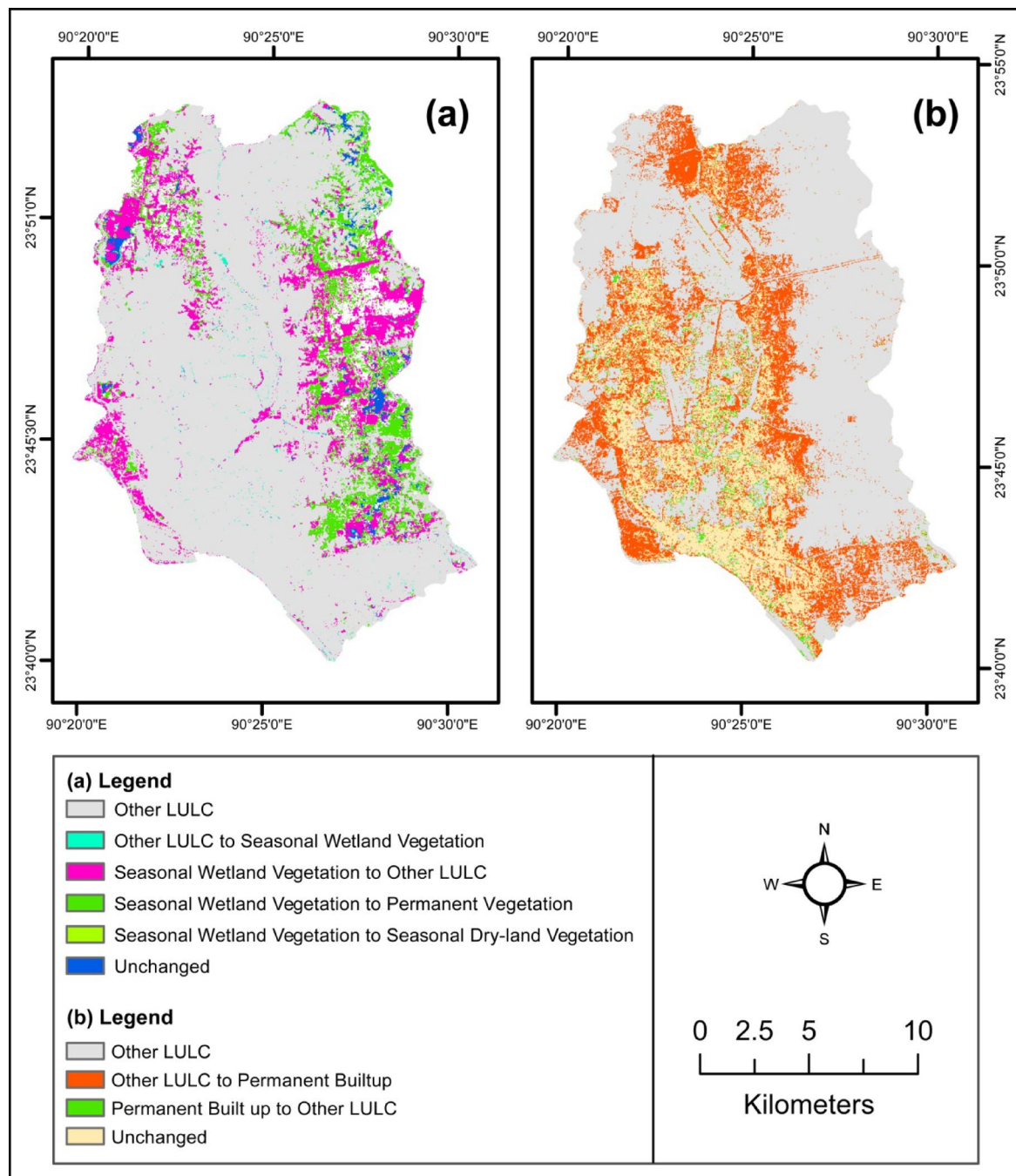


**Fig. 5.** LC change map between year 2000 and 2022, (a) exchange of seasonal wetland vegetation and (b) exchange of permanent built up areas. Maps were generated using QGIS 3.26.1 (QGIS Development Team, <https://qgis.org>) and ArcGIS 10.5 (Esri, <https://www.esri.com>).

## Discussions

### Impact of seasonality in LC variations

The findings of the research indicate distinct seasonal variations in LCs in Dhaka City (Table 1; Fig. 4) along with temporal variation (Table S 4 and Fig. 4). The unique geographical location, climate and dynamic weather pattern across seasons and the diverse ecosystems of Dhaka make it a thriving place for biodiversity offering diverse natural phenomena<sup>42</sup>. The distinct characteristics of deciduous trees in Dhaka<sup>6,43,44</sup> contribute to the increase in the spatial extent of vegetation in growing seasons, especially in post-monsoon, and decrease in dry seasons, which is evident in the recent year (2022) in current research (Figs. 2 and 4). However, an increase in vegetation during dry seasons was evident in 2000 and 2010. Because, the lowland around Dhaka is extensively used for agricultural activity or covered by dense grasses mainly by catkin (a flowering spike of trees such as willow and hazel) during dry seasons whereas, during the rainy season, these areas remain underwater<sup>39,40,45</sup>.

Moreover, the permanent and seasonal wetlands and landfill sites in the southern and northern parts of Dhaka city<sup>6</sup>, show seasonal variations, remaining underwater in post-monsoon, being covered by vegetation during winter, and becoming barren during summer (Fig. 3); contributing in seasonal change in LCs. Additionally, the increase in roadside trees and rooftop gardening<sup>40</sup>, significantly affects the seasonal vegetation cover, making complexity in demarcating the built-up and vegetation cover and increasing the mixed urban areas in recent times (Figs. 2 and 4). In the current research, most of the seasonal variation has been evident in the wetland areas and vegetation covers whereas built infrastructure has shown comparatively minor variation (Table 1; Figs. 2 and 4).

### Socio-economic factors responsible for SILC change

In the last few decades, a large amount of LC exchange has occurred in and around Dhaka City due to the significant modification of the land surface driven by unplanned urban growth. A significant landfilling was conducted in and around Dhaka city for commercial and residential housing purposes which ultimately affected wetlands in diverse aspects<sup>6,22,46–50</sup>. Sometimes wetlands are left for a few years after being filled. They are then overgrown with grass or plants or used for agricultural purposes so that it is identified as permanent vegetation or bare land for the next few years. This type of change largely contributed to an increase in seasonal dry-land vegetation and permanent vegetation driven by seasonal wetland vegetation (Fig. 5). From Fig. 4, it is evident that from 2000 to 2010 wetlands significantly altered into vegetation or bare land due to landfilling and this trend is also followed in the next decade between 2010 and 2022. During this time, the filled areas were gradually being converted into built-up on all sides (Fig. 5). Moreover, the addition of Dhanmandi Lake<sup>51</sup> and some other artificial lakes and ponds in some newly developed residential areas slightly contributed to seasonal water bodies or wetland or dry land vegetation (Figure S1–4)<sup>15,40,52–54</sup>. Slums of the city were also destroyed and relocated for residential and housing purposes which temporarily contributed to a slight increase in greener or bare areas (Figure S 1 and 2). Additionally, Uttara and Gulshan model towns, and Badda Demra, Kurmitola, Bashundhara Baridhara and Pallabi housing areas have contributed in addition to some seasonal dry-land vegetation seasonal built-up and mixed urban areas (Fig. 4)<sup>15,40,53</sup>. According to Parvin et al. (2018)<sup>55</sup>, there is 9.2 sq km of single-cropped area, 94.5 sq km of double-cropped area and 5.7 sq km of triple-cropped area in Dhaka Sadar Upazila. This cropping is practised in the wetlands and low-lying areas of Dhaka which become arable during dry seasons. This significantly alters the seasonal land cover pattern across the city which is also evident in the current research.

### Adopted policy changing SILC in Dhaka City

Besides increasing seasonal variation, government and private initiatives (policy, projects and plans) have increased greener spaces in Dhaka City in the last few decades although the amount is minor. Dhaka city corporations have undertaken beautification projects to plant trees in different parts of DMP<sup>56</sup>. Several trees have been planted in road divides or alongside the roads slightly converting bare land and built-up areas into vegetation which is evident in the captured satellite images<sup>57,58</sup> and in the classified maps of current research (Fig. 2). Dhaka South City Corporation made 217.38 km of footway into an urban forest structure by planting different street tree species<sup>59</sup>, which have converted some built-up areas into vegetation and bare land over the study time evident in the classified maps (Fig. 2). According to Nawar (2022)<sup>40</sup>, between 1989 and 2020 Dhaka City gained 20.71 sq km of green space due to several government and private initiatives like the Dhaka city beautification project, roadside tree plantation project, and rooftop gardening. These roadside trees and rooftop gardening<sup>40</sup> have a significant impact on seasonal variation in vegetation cover<sup>44</sup> and long-term vegetation gain<sup>40,59</sup> which is evident in the current research (Figs. 2, 4 and 5). In 2014, 170 acres of land have been added by removing 2,000 structures from the Korail slum in Dhaka city<sup>60</sup>. This area has been converted into green space from built-up areas as this is under the planning of development<sup>60</sup>. This has converted some barren land and built-up areas into vegetation cover across the city (Table 1; Fig. 4), which was also evident in the previous research conducted on Dhaka City and Dhaka district<sup>18,25,41,56</sup>. Re-excavation of Hatir Jheel (Figure S 7 and 9) and Begunbari Canal has increased the water detention capacity of Dhaka from 1.4 sq km to 2.20 sq km<sup>61</sup>, which ultimately increased the areas of permanent water bodies in the classified maps (Figs. 3 and 4). Some barren areas around Hatirjheel and Dhanmandi Lake have been converted into green spaces due to the beautification projects. Additionally, the conversion of built-up and bare land to other types of LC was also evident. Several tree plantation projects undertaken by city corporations and the activities of developer companies in housing areas have contributed to a slight increment in vegetation cover in the city; although limited discussion was found for these types of change as these are minor<sup>56</sup>.

### Comparison of LC and SILC with previous research

Previous studies reported a significant seasonal variation in vegetation covers, low-lying areas, wetlands and water bodies identified from satellite image analysis and LC mapping<sup>41,45</sup>, changing the spatial extent of classified areas of LCs in different seasons of a single year<sup>18,25,41,45,56</sup>. These types of changes are also evident in the current research (Table 1; Fig. 2). Mia et al. (2017)<sup>62</sup> identified a few seasonal vegetated lands in Dhaka city studying the images of the pre-monsoon period which supports the findings of the current research. The conversion of wetlands and seasonal fluctuation of the LC in the east and west sides of Dhaka city found in the current research aligns with the findings of Dewan & Yamaguchi (2009a & 2009b)<sup>6,46</sup> Imran et al. (2021)<sup>24</sup> and Moniruzzaman et al. (2020)<sup>38</sup>; although classification scheme and the acquired date of analyzed satellite images are different. Such as Dewan & Yamaguchi (2009a & 2009b)<sup>6,46</sup> and Moniruzzaman et al. (2020)<sup>38</sup> used satellite data for the winter season and Imran et al. (2021)<sup>24</sup> used the summer season. Dewan & Yamaguchi (2009a)<sup>6</sup> found that between 1992 and 2003 cultivated land (6.7%) has been increased in Dhaka city. This type of change is also evident in the current research, such as the shift of agricultural land to the filled wetland mostly on the east side of the

city (Figs. 4 and 5). Ahmed (2011)<sup>45</sup> and Ahmed & Ahmed (2012)<sup>41</sup> analysed the LC change between 1989 and 2009 and identified slight decreases in built-up areas (around 2% of the total area) to other types of LC although a significant increase in built-up areas has occurred within the studied time<sup>45</sup>. Kafy et al. (2021c)<sup>56</sup> prepared LULC using rapid eye images between the years 2012 and 2018 where the rejuvenation of Hatirjheel Lake and Dhanmandi Lake was evident which increased some permanent water bodies in Dhaka City.

The conversion of barren areas into vegetation cover, especially around Hatirjheel and Dhanmandi was also evident in Kay et al. (2021a & c)<sup>25,56</sup>. Sresto et al. (2022)<sup>18</sup> assessed the seasonal LC of Dhaka and measured the summer-winter variation of LC of Dhaka district where LC exchange among every class was evident. A significant conversion of built-up areas to agricultural land, bare land, vegetation, and water bodies has been documented both within a single year and over the long term<sup>18</sup>. However, the current research identified only a minor conversion of built-up areas to other LC categories.

### Application of SILC in urban sustainability, climate resilience, and policy planning

The proposed method, generated data, results and findings of the current research have some robust applications in the urban sustainability, climate resilience, and policy planning of Dhaka city. The integration of the seasonal LC map, termed as SILC, provides a baseline dataset of three consecutive years 2000, 2010 and 2022, which depicts the existing and previous state SILC of Dhaka City. The change detection from SILC helps to identify the ecologically vulnerable zones along with urban growth patterns with rapid development (Fig. 2.a-c and 5.a and 5.b). Moreover, the SILC provides information about the transformation of different land use zones of the city over time. This information is the foundation for effective urban planning, infrastructure development, and environmental conservation planning and policy formulation of the city.

Areas with permanent built-up have minimal green open spaces with minor trees, located in the city centre (Figs. 4 and 5), resulting in higher health hazards, and extreme urban heat island effects<sup>63</sup> and are highly vulnerable to heat waves and flooding in future due to climate change<sup>64,65</sup>. According to Fig. 5, these areas are expanding in the peripheral areas in recent times. Additionally, increased population, traffic and waste in these areas (Fig. 4) further degrade the scenario. Moreover, heavy drainage congestion and urban flooding are already evident in those areas of Dhaka City<sup>61,66,67</sup>, which will degrade in future due to climate change-driven extreme temperature and rainfall<sup>61,64,65</sup>. Therefore strong regulatory policy should be implemented to increase drainage, waste management and traffic control to increase the coping capacity and climate resilience of the city<sup>68,69</sup>. In and around permanent built-up areas, increasing tree plantation around the house, rooftop gardening, increasing artificial reservoirs and re-excavation of channel will contribute to reducing extreme heat during summer and will increase the climate resilience of the city. Additionally, immediate conservation planning should be taken in mixed urban and seasonal urban areas, because of their potential to reduce heat compared to permanent built-up areas<sup>63,70–72</sup>.

Special focus should be given to rejuvenating drainage to reduce urban flooding in these particular areas<sup>10,37,73–75</sup>. Re-excavated water bodies, such as Hatir Jheel and Begunbari Canal, should be monitored on a regular basis<sup>40,61</sup>. This type of re-excavation should be conducted in the areas of seasonal water bodies, seasonal bare lands, and seasonal dry-land vegetation to increase the discharge and water retention capacity of Dhaka city (Figs. 2 and 5) which will increase climate resilience during extreme rainfall and temperature events. The areas converting into urban or bare land should be monitored and proper development planning should be implemented for sustainable horizontal and vertical development of the city. The areas covered by seasonal vegetation or seasonal bare land should be used to increase green spaces and drainage to reduce the risk of urban heat island effect<sup>63,71</sup> and urban flooding<sup>73,74</sup>. It is also seen that a large amount of wetland vegetation has been transformed into other types of SILC such as vegetation and bare land, especially in the northern and southern parts of the city. Policy can be taken to convert them again to water bodies. In the areas of permanent vegetation, tree plantation should be increased even if possible by adding mud from other areas. The natural biological and ecological processes have been significantly affected and the ecological habitats have been lost on the east and west sides of the city due to SILC alteration driven by anthropogenic processes (Fig. 5). Moreover, built-up areas are expanding on all sides by converting all types of LCs (Fig. 5.b). This urban expansion should be strongly regulated and sometimes stopped to protect the different types of vegetation and water bodies. Besides, during building construction extra space should be kept to plant at least some small trees. The housing which is under construction now should be under strong policies and regulations to keep adequate open green space and parks to mitigate future risk<sup>71</sup>. In Table 2, some specific recommendations and solutions have been given incorporating the prepared LC maps for Dhaka City.

### Conclusion

The findings of the research demonstrated the significance of using seasonal LCs to address the challenges and limitations of single-date satellite images in accurately representing LC dynamics. By integrating LCs of three seasons of a single year, the study developed improved Seasonal Integrated Land Cover (SILC) maps for 2000, 2010 and 2022, providing a more reliable representation of Dhaka City's dynamic urban landscape. The LC change detection derived from LC maps indicated that due to rapid urbanization, all types of vegetation cover and water bodies are converting into built-up and bare lands at an alarming rate. Besides, due to the complex land use patterns, heterogeneity increased in Dhaka city affecting the spectral signature of the satellite image creating complexity in demarcating LC classes. These insights are crucial for guiding sustainable urban planning, climate resilience and policy-making by identifying ecologically vulnerable zones and monitoring urban expansion trends.

The study has direct policy implications for urban planners. The SILC-based approach can support zoning regulations, infrastructure development, climate resilience, and flood risk and urban heat island mitigation by distinguishing between permanent and seasonal land covers. Urban planners can use these findings and the

SILC Type	Policy recommendation/solution
Permanent built-up	<ul style="list-style-type: none"> <li>• Improve drainage infrastructure and clear occupied canals.</li> <li>• Ensure proper waste management with adequate dustbins based on population density.</li> <li>• Control traffic to increase the coping capacity of the city and reduce air pollution in the densely populated areas.</li> <li>• Clear the garbage and silt from the canals and ensure interlinkages with the main river.</li> <li>• Clear roadside drains to increase water flow to reduce waterlogging.</li> <li>• Introduce permeable pavements in dense urban areas.</li> </ul>
Wetland vegetation	<ul style="list-style-type: none"> <li>• Halt the conversion into other land cover types.</li> <li>• Regularly monitor wetland areas using LC maps.</li> <li>• Develop policies to restore wetlands and reconvert degraded areas into water bodies.</li> </ul>
Mixed urban and seasonal urban areas	<ul style="list-style-type: none"> <li>• Implement immediate conservation planning.</li> </ul>
Permanent and seasonal water bodies	<ul style="list-style-type: none"> <li>• Take immediate steps for re-excavation.</li> <li>• Regularly monitor restored areas, like Hatir Jheel and Begunbari Canal.</li> </ul>
Seasonal water bodies, seasonal bare lands, seasonal dry-land vegetation	<ul style="list-style-type: none"> <li>• Re-excavate these areas to increase Dhaka city's discharge and infiltration capacity.</li> <li>• Increase groundwater recharge potential.</li> </ul>
Seasonal bare lands, seasonal dry-land vegetation	<ul style="list-style-type: none"> <li>• Implement biopore infiltration holes, a technique used in Indonesia, can be applied in these areas, to reduce the risk of urban flooding and drainage congestion.</li> </ul>
Seasonal vegetation and seasonal bare land	<ul style="list-style-type: none"> <li>• Expand green spaces and drainage systems to mitigate urban heat island effects and urban flooding even in the future climate change.</li> </ul>

**Table 2.** Strategies and recommendations for sustainable development policy of Dhaka City based on SILC.

prepared SILC maps to enhance green space preservation, improve drainage systems, and implement targeted conservation efforts in mixed and seasonal urban areas to strengthen climate resilience and urban sustainability.

However, some limitations of the research methods must be acknowledged. The classification accuracy largely depends on the quality of single-date seasonal maps, and the study relies on medium-resolution satellite images (Landsat 5 and 8 OLI), which may not capture fine-scale land cover details like the sentinel image. Additionally, the spectral indices were not used in this research, which has been used in some research to reduce classification uncertainties. Spectral similarities between land cover types, particularly during dry seasons, may create bias in classification accuracy. For example, bare land and built-up areas may exhibit similar spectral reflectance, leading to misclassification. Additionally, seasonal variations in vegetation cover could influence classification results, as some vegetation types may appear differently depending on moisture levels, thermal effect and phenological cycles.

The current research utilized four basic LC classes; incorporating a greater variety could enhance the reliability and applicability of LC maps. However, this may also introduce complexities in explaining and managing SILC during practical applications. The LC classes largely depend on the geographical context, vegetation type, and rainfall pattern of the study area, as a result, different locations may increase or decrease final LC classes. As a result, in-depth knowledge about the study area will be required during replication of the method. Future research should explore higher-resolution satellite imagery (e.g., Sentinel-2, commercial satellite data) and advanced machine-learning techniques for improved classification accuracy. Expanding the classification to include more detailed LC categories could be tested whether they enhance the practical applicability.

## Materials and methods

### Study area

Dhaka is the capital of Bangladesh, located between 23° 40' N to 23° 54' N latitude and 90° 20' E to 90° 28' E east longitude (Fig. 6). The administrative unit of the Dhaka Metropolitan (DMP) area is considered for the research<sup>24,33,35,76</sup>. It is one of the fastest-growing megacities and densely populated areas in the world. The population of Dhaka was 14.4 million in 2011 and it is continuously growing. To meet the needs of the ever-growing population several development activities largely increased which led to the conversion of natural landscapes into built infrastructure<sup>76</sup>. A number of small to large parks and playgrounds in the city core allow diverse vegetation patterns along the built infrastructure<sup>77</sup>. Besides, several small water bodies (ponds, lakes and river channels) located in the city core increased the diversity in the land cover pattern. Due to excessive population pressure vegetation and water bodies are under threat of conversion into built-up areas or bare land<sup>25,34</sup>. High urbanized areas of the city are located in the central and southern parts of the city<sup>24</sup>.

On the east and north-west side, some marshlands and agricultural lands are located<sup>24</sup> which vary following the seasonal climatic pattern. The expanded roads in the city increased the area's complex impervious surfaces subsequently increasing the urban heat island effect and leading to an unhealthy environment in the city<sup>78,79</sup>. The location in the sub-tropical monsoon climate affects the land cover of Dhaka city due to the presence of seasonally varying vegetation patterns, expansion or shrinking of water bodies, alteration of water bodies by water-born vegetation, and alteration of low or fellow lands into agricultural lands<sup>25,39</sup>. As a result, the land cover (LC) of Dhaka City needs to be studied by considering the seasonal LCs rather than studying single-date LC.

### Methodological flow

The acquired satellite images were pre-processed and supervised image classification of random forest was applied to classify the LC of each month of every year. The accuracy of each of the classified images was tested by preparing a confusion matrix. LC of three seasons of each year was combined into a single map using overlay technique and again these are re-classified according to the seasonal rotational pattern of LC classes. A change detection technique was applied to measure the change of LC in two successive years. The LC change matrix

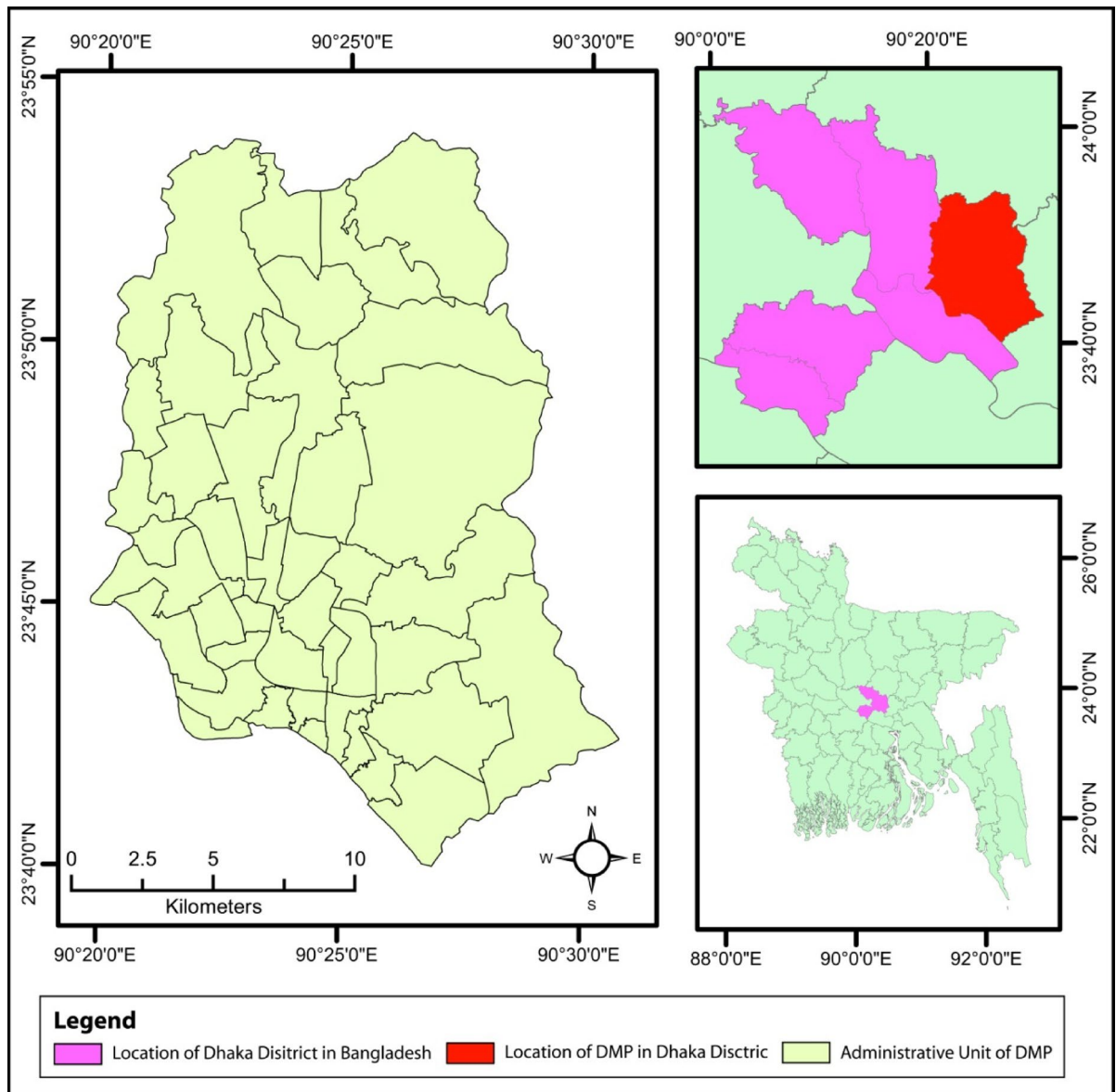


**Fig. 6.** Location of the study area. The figure in the right panel shows the administrative boundary of the Dhaka Metropolitan (DMP) which has been mentioned as Dhaka City in the manuscript.

was prepared to assess and visualize the LC changes and their drivers in Dhaka city. The broad steps followed in the research, from preparing actual LC from seasonal LC to measuring LC change, are shown in the flow chart below (Fig. 7).

#### Data and data source

Landsat 5 TM and Landsat 8 OLI satellite images were collected from the USGS server. The selection of Landsat images over higher-resolution datasets like Sentinel-2 was driven by the requirement for consistent temporal coverage over the long study period (2000, 2010, and 2022). Although the Sentinel-2 image offers higher spatial resolution, its historical record starts from 2015, making it less suitable for long-term LC change analysis. The spatial resolution of the Landsat 5 TM and 8 OLI images is 30 m, suitable for capturing broad LC changes in an urban setting along with maintaining temporal consistency for change detection. The selection also aligns with key urban planning milestones in Dhaka, such as the Dhaka Metropolitan Development Plan (1995–2015) (RAJUK 1995)<sup>80</sup> and the Revised Structure Plan (2016–2035) (RAJUK 2015)<sup>81</sup>, which allow assessment of land cover change across planning cycles. Cloud-free images (0.2% < cloud) were collected for three seasons of post-monsoon, winter and summer seasons for all the study years. The image acquisition dates are shown in Table 3.

The seasonal images were selected based on the meteorological seasons of Bangladesh. In Bangladesh, the post-monsoon season includes October and November, winter spans from December to February, and summer extends from March to May<sup>18–22,43,82,83</sup>.

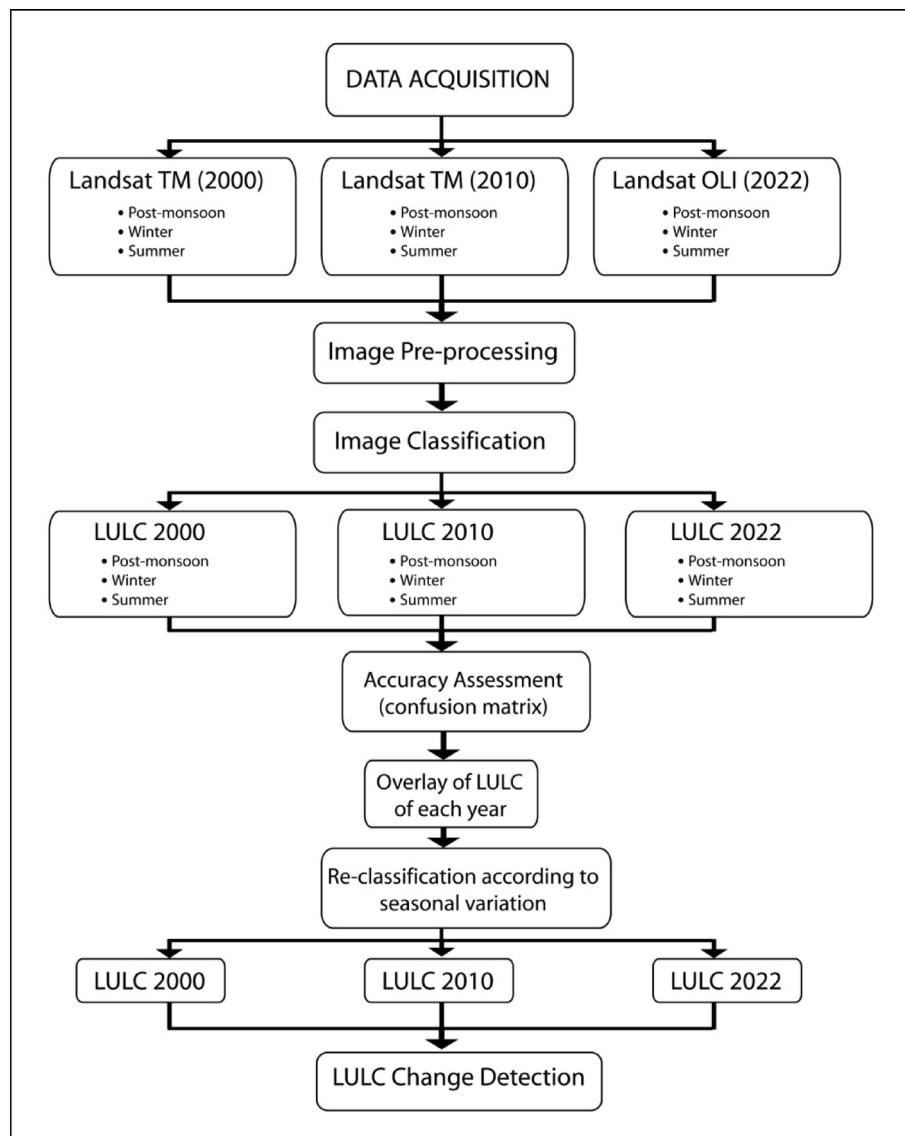


**Fig. 7.** Methodological flow of the research.

Seasons	2000 (Landsat 5 TM)	2010 (Landsat 5 TM)	2022 (Landsat 8 OLI)
Post-monsoon	28/10/1998	2010/11/30	2021/11/28
Winter	19/01/2000	2011/01/01	2022/1/07
Summer	21/03/1999	2011/04/07	2022/03/20

**Table 3.** Image acquisition date.

### Image pre-processing

#### *Radiometric calibration and atmospheric correction*

Radiometric calibration and atmospheric correction of the satellite images have been conducted using the DOS-1 Atmospheric Correction method in the Semi-Automatic Classification Plugin (SCP) of QGIS software<sup>84</sup>. DOS-1 method showed higher performance over the darker surfaces of water and artificial turf and sand cover compared to other models in Landsat images, even for spectral signature analysis and spatial profile of vegetation index, where ground-based samples were used for validation<sup>85–88</sup>. Researchers also found minor differences in the performance of 6 S, DOS1, FLAASH, and ACOLITE models showed negligible variation<sup>84,89</sup>. As a result, DOS-1 has been frequently used by researchers to compare the results of time series satellite images<sup>88,90,91</sup>. In this research DOS-1 method of SCP Plugin of QGIS 3.26.1 software has been used. The atmospheric correction process of DOS-1 in QGIS involves the following steps:

1. Radiometric Calibration (DN to Radiance): In this step digital numbers (DNs) are converted to at-sensor radiance ( $L_{\text{sensor}}$ ) using the following Eq. (1):

$$L_{\text{sensor}} = G_{\text{rescale}} * DN + L_{\text{bias}} \quad (1)$$

Where,  $L_{\text{sensor}}$  = Radiance at the sensor (in  $W/m^2/sr/\mu m$ ),  $G_{\text{rescale}}$  = Rescaling gain factor, DN = Digital number from the satellite image,  $L_{\text{bias}}$  = Minimum radiance (bias) or radiance offset.

2. Estimation of Atmospheric Path Radiance (Haze Radiance): After performing radiometric calibration atmospheric path radiance is calculated, that accounts for the scattering of sunlight in the atmosphere. In DOS-1 method, the darkest pixels in the satellite image (such as water bodies or shadows) are identified as objects with near-zero reflectance. These near zero pixels are used to account the haze radiance in the satellite image. The haze radiance,  $L_{\text{haze}}$  in the Eq. 2, is measured based on the minimum radiance value observed in each band of the satellite image:

$$L_{\text{haze}} = L_{\text{min}} - \quad (2)$$

It is assumed that  $L_{\text{haze}}$  value represents the atmospheric contribution into the image, which further subtracted from the sensor radiance.

3. **Dark Object Subtraction (DOS-1): Atmospheric Correction:** Once the haze radiance has been estimated, the Dark Object Subtraction (DOS-1) formula (equation-3) is employed to correct for atmospheric path radiance.

$$L_{\text{corrected}} = L_{\text{sensor}} - L_{\text{haze}} \quad (3)$$

Where,  $L_{\text{corrected}}$  = Radiance after subtracting the atmospheric path radiance,  $L_{\text{sensor}}$  = Radiance at the sensor (from the DN to radiance conversion),  $L_{\text{haze}}$  = Atmospheric path radiance (haze radiance) estimated from dark objects.

4. **Conversion of Corrected Radiance to Surface Reflectance:** Finally, equation-4 has been used to convert the corrected radiance values to surface reflectance.

$$\rho = \frac{\pi * L_{\text{corrected}} * d^2}{E_{\text{sun}} * \cos(\theta_s)} \quad (4)$$

Where,  $\rho$  = Surface reflectance (dimensionless),  $L_{\text{corrected}}$  = Corrected radiance (after DOS-1),  $d$  = Earth-Sun distance (in astronomical units),  $E_{\text{sun}}$  = Exoatmospheric solar irradiance for the specific wavelength (can be found in metadata),  $\theta_s$  = Solar zenith angle, which can be calculated as:

$$\theta_s = 90^\circ - \text{Solar Elevation Angle} \quad (5)$$

The position of the sun in the sky at the time of image capture is taken into account by the solar zenith angle, which has significant impact on the amount of radiation that reaches the Earth's surface.

### Land cover classification technique

The LC was classified using the machine learning algorithm of Random Forest which is very popular and is widely accepted by practitioners in the field of LC classification<sup>15,92-95</sup>. Random Forest is an ensemble machine-learning algorithm that uses a number of decision trees to enhance the accuracy and robustness of the classification by minimizing overfitting and increasing generalization. As a result, the RF algorithm is very effective for land cover (LC) mapping as it can handle high-dimensional datasets, reduce overfitting, and provide estimates of variable relevance. In QGIS, the RF classifier is implemented in the Semi-Automatic Classification Plugin (SCP), which automates feature selection, training, and classification. The algorithm executes by randomly selecting subsets of training samples and creating several decision trees based on this. Each tree individually classifies the data, and the final classification is chosen by a majority vote among the trees. The RF classifier follows this general equation:

$$y = \text{mode}(f_1(x), f_2(x), f_3(x) \dots \dots \dots f_n(x)) \quad (6)$$

Where,  $y$  = predicted class label,  $f_i(x)$  = the classification result from the  $i^{\text{th}}$  decision tree,  $n$  = total number of decision trees. The final output is determined by the majority class (mode) across all trees.

Four main LC categories namely Water, Vegetation, Built-up, and Bare Land were selected for classifying Landsat images of each season (Table 4). Training samples for LCs were carefully selected through detailed visual analysis. True-color and various false-color composite images were tested to ensure accurate selection of the sample. Additionally, some locations were cross-validated using ground truth data collected from field surveys and Google Earth imagery. Coordinates of stable landmarks such as the Sangshad Bhaban, Baldha Garden, Bangladesh National Zoo, Ramna Park, Hatirjheel Lake, Dhanmondi Lake, and parts of Old Dhaka were used for both image classification and classified map validation. These locations were selected because of their consistent land cover characteristics since 2000. Their coordinates were used to verify classified outputs across all years, and especially for 2022, these areas were cross-checked with actual ground conditions. To understand the seasonal pattern of land cover, geographical context was considered during classification and validation. In addition, high-resolution imagery from Google Earth Pro was used as a supplementary source to visually validate selected areas of the classified maps across different seasons and years.

LC Type	Description	False-color composites
Water	Rivers, ponds, canals, wetlands.	Dark blue to black in NIR-SWIR combinations.
Vegetation	Forests, dense and scattered trees, grass, bushes, urban parks, roadside greenery, scattered agricultural lands.	Bright green in NIR (band 4) and red (band 3) combinations.
Built-up	Residential, commercial, and industrial areas, high-rise buildings, roads, and infrastructure.	White to gray in NIR (band 4) and SWIR (band 5) combinations.
Bare Land	Construction sites, vacant plots, land development areas, bare surfaces.	Brown to light gray in NIR (band 4) and SWIR (band 5) combinations.

**Table 4.** Classification criteria of LC.

The quantitative accuracy of the classified maps was assessed using a confusion matrix by calculating standard classification metrics, including User Accuracy (UA), Producer Accuracy (PA), Overall Accuracy (OA), and the Kappa Coefficient (Kc)<sup>96</sup>. User Accuracy (UA) (Eq. 7) refers to the proportion of correctly classified samples for a given class relative to the total number of samples classified in that class, indicating commission error. Producer Accuracy (PA) (Eq. 8) represents the proportion of reference (ground truth) samples that are correctly classified, reflecting omission error. Overall Accuracy (OA) (Eq. 9) denotes the ratio of correctly classified samples across all classes to the total number of reference samples. The Kappa Coefficient (Kc) (Eq. 10) measures the agreement between the classified map and the reference data while accounting for the possibility of agreement occurring by chance, thus providing a more robust assessment of classification performance.

$$UA = \frac{x_{ii}}{x_{i+}} \quad (7)$$

$$PA = \frac{x_{ii}}{x_{+i}} \quad (8)$$

$$OA = \frac{\sum_{i=1}^k x_{ii}}{N} \quad (9)$$

$$Kc = \frac{N \sum_{i=1}^k x_{ii} - \sum_{i=1}^k x_{i+} x_{+i}}{N^2 - \sum_{i=1}^k x_{i+} x_{+i}} \quad (10)$$

Where,  $x_{ii}$  = number of correctly classified samples for class  $i$ ,  $x_{i+}$  = total samples classified as class  $i$  (row total),  $x_{+i}$  = total reference samples for class  $i$  (column total),  $N$  = total number of samples,  $k$  = total number of classes.

### Seasonally integrated land cover (SILC)

The classification was conducted for each of the seasonal images of each year, and the three classified maps of each year were combined using the overlay method in ArcMap 10.5 software. The combined map derived from the overlay was reclassified according to the seasonal rotational pattern of the LC following the codes generated in the attribute field (Fig. 7). Besides, a manual search of each rotational LC was cross-checked from the false colour combination of the raw composite images. Ground truth data were incorporated using high-resolution imagery and field verification points where available.

During the reclassification, the SILC categories were defined based on urban environmental characteristics and seasonal changes in Dhaka (Table 5). The classification scheme included permanent and seasonal classes. If the code was 111 (Fig. 8), it is classified as permanent water body followed by 222 as permanent vegetation, 333 as permanent built-up, and 444 as permanent bare land. When LC pixels change in subsequent seasons, the pixels are reclassified according to that change by considering the geographical context of the region. Such as 112 = Seasonal Wetland Vegetation, 424 = Seasonal Bare land, 324 = Mixed Urban etc. The full reclassification of both codes and labels is supplied in Table S 5. The final SILC classification map consists of eleven standardized classes, defined as follows (Table 5):

### Change detection analysis

To accurately analyze land cover (LC) transitions over successive periods (2000–2010, 2010–2022, and 2000–2022), a pixel-by-pixel cross-tabulation change detection technique was employed (Islam et al. 2021). A change matrix was generated to quantify transitions between LC categories and identify their primary driving factors.

#### Accuracy assessment

LC of three seasons of post-monsoon, winter and summer are prepared for the year 2000, 2010 and 2022 (Fig. 2.a to 2.i). The accuracy of the maps is shown in Table 6. The accuracy of the classified maps is tested using user accuracy, producer accuracy, overall accuracy and kappa coefficient<sup>96–102</sup>. An error matrix for each of the maps is also prepared. The accuracy assessment has been done using the “Compute Confusion Matrix” tool of ArcMap 10.5 software<sup>103,104</sup>. The overall accuracy and the Kappa coefficient of all the maps are above 0.95 indicating a very good accuracy of the classified maps<sup>98,99,102,105</sup>. The user accuracy and producer accuracy of all the seasonal maps also showed very good agreement. Considering the strong classification performance achieved using the original reflectance bands ( $OA > 0.95$ ) and integration limitations in QGIS, spectral indices were intentionally excluded from the classification model.

SILC Class	Definition
Permanent Water Body	Areas are consistently classified as water in all three seasons of the year. These are perennial wetlands or water bodies, including rivers, lakes, ponds, and perennial wetlands with year-round water presence (e.g., code 111).
Seasonal Wetland Vegetation	Wetland areas that exhibit seasonal vegetation growth, typically submerged or waterlogged during monsoon and vegetated during dry seasons (e.g., codes 112, 114, 124, 141).
Mixed Water	Transitional zones that alter between water and other LC classes (bare land, vegetation, impervious surface) across seasons, often found along riverbanks, wetlands, or drainage channels (e.g., codes 123, 134, 421).
Seasonal Bare Land	Areas classified as bare land in one or more seasons but not consistently, often representing fallow lands, construction sites, or exposed soil surfaces that change across the seasons (e.g., codes 133, 144, 424, 444).
Seasonal Dry-land Vegetation	Areas covered by agricultural fields, grasslands, or dry open spaces that are green and vegetated only during part of the year (typically winter or post-monsoon), turning brown or bare during summer (e.g., codes 211, 221, 422).
Mixed Vegetation	Areas that alter between different vegetation states across seasons, such as areas with partial tree cover, rooftop gardening, and deciduous trees along or over the impervious surfaces (e.g., codes 213, 231, 234, 243).
Permanent Vegetation	Areas remain densely vegetated across the year, including forests, planted social forestation, urban parks, urban green spaces and perennial green cover (e.g., code 222).
Seasonal Built-up	Urban or semi-urban areas that exhibit built-up characteristics during one or two seasons, potentially due to temporary structures, changing land use, or urban shadowing (e.g., codes 313, 331, 334, 433).
Mixed Urban	Pixels that fluctuate between built-up and other classes (e.g., vegetation, bare land) across seasons. These are typically fringe or transforming zones undergoing rapid urbanisation (e.g., codes 321, 324, 341, 431).
Permanent Built-up	Areas that are consistently classified as built-up in all three seasons, including dense urban settlements, commercial zones, roads, and infrastructure (e.g., code 333).
Permanent Bare Land	Lands that remain bare and devoid of vegetation or built-up features throughout the year, often representing barren land, dry patches, or exposed soil (e.g., code 444).

**Table 5.** Definition of SILC classes.

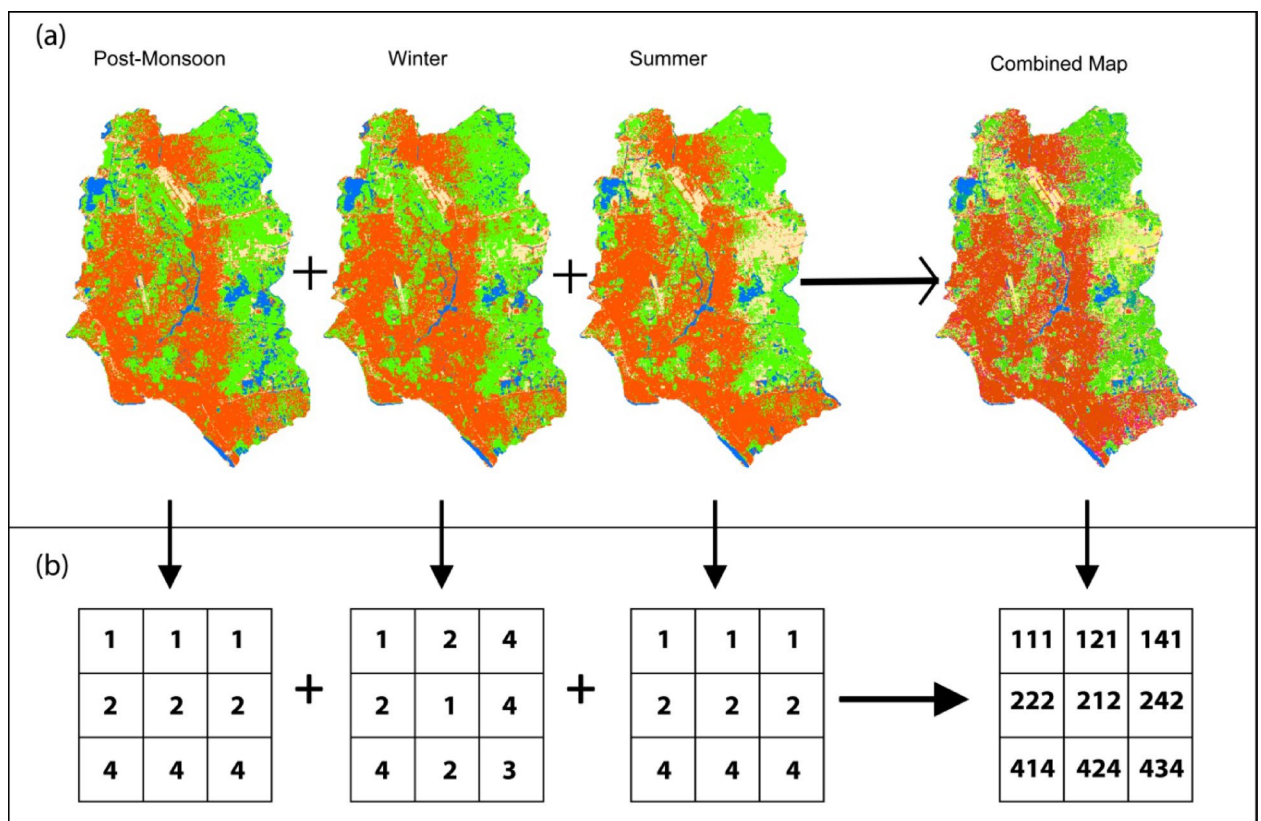


**Fig. 8.** Pixel by Pixel overlay of the classified images of the seasons and their reclassification. This figure shows the reclassification process and mechanism to prepare the final LC map by using the seasonal LCs. Maps were generated using QGIS 3.26.1 (QGIS Development Team, <https://qgis.org>) and ArcGIS 10.5 (Esri, <https://www.esri.com>), then refined using Adobe Illustrator CS (version 11.0.0, Adobe, <https://www.adobe.com>).

Year	Season	Class value	C_1	C_2	C_3	C_4	Total	UA	OA	Kc
2000	PM	C_1	52	0	0	0	52	1	0.99	0.98
		C_2	0	51	0	1	52	0.98		
		C_3	0	0	50	1	51	0.98		
		C_4	0	0	1	46	47	0.98		
		Total	52	51	51	48	202	0		
		PA	1	1	0.98	0.96	0			
	Winter	C_1	51	1	0	0	52	0.98	0.97	0.96
		C_2	0	51	1	1	53	0.96		
		C_3	0	0	53	1	54	0.98		
		C_4	1	0	1	49	51	0.96		
		Total	52	52	55	51	210	0		
		PA	0.98	0.98	0.96	0.96	0			
	Summer	C_1	52	0	0	0	52	1	0.97	0.96
		C_2	0	43	0	1	44	0.98		
		C_3	0	0	52	1	53	0.98		
		C_4	0	2	2	57	61	0.93		
		Total	52	45	54	59	210	0		
		PA	1	0.96	0.96	0.97	0			
2010	PM	C_1	47	0	1	0	48	0.98	0.98	0.97
		C_2	0	51	0	2	53	0.96		
		C_3	1	0	52	0	53	0.98		
		C_4	0	0	1	50	51	0.98		
		Total	48	51	54	52	205	0		
		PA	0.98	1	0.96	0.96	0			
	Winter	C_1	47	1	0	0	48	0.98	0.97	0.96
		C_2	0	49	1	1	51	0.96		
		C_3	1	0	51	0	52	0.98		
		C_4	0	1	1	52	54	0.96		
		Total	48	51	53	53	205	0		
		PA	0.98	0.96	0.96	0.98	0			
	Summer	C_1	42	1	0	0	43	0.98	0.97	0.96
		C_2	1	55	0	1	57	0.96		
		C_3	1	0	51	1	53	0.96		
		C_4	0	0	1	51	52	0.98		
		Total	44	56	52	53	205	0		
		PA	0.95	0.98	0.98	0.96	0			
Continued										

Year	Season	Class value	C_1	C_2	C_3	C_4	Total	UA	OA	Kc
2022	PM	C_1	46	0	1	0	47	0.98	0.98	0.97
		C_2	0	43	0	0	43	1		
		C_3	0	0	118	1	119	0.99		
		C_4	0	1	2	41	44	0.93		
		Total	46	44	121	42	253	0		
		PA	1	0.98	0.98	0.98	0			
	Winter	C_1	46	0	0	0	46	1	0.98	0.97
		C_2	0	44	3	0	47	0.94		
		C_3	0	0	116	0	116	1		
		C_4	0	0	2	42	44	0.95		
		Total	46	44	121	42	253	0		
		PA	1	1	0.96	1	0			
	Summer	C_1	46	0	0	0	46	1	0.98	0.97
		C_2	0	43	0	0	43	1		
		C_3	0	0	120	3	123	0.98		
		C_4	0	1	1	39	41	0.95		
		Total	46	44	121	42	253	0		
		PA	1	0.98	0.99	0.93	0			

**Table 6.** Accuracy of the classified maps (Table Legend: C\_1 = Water, C\_2 = Vegetation, C\_3 = Built up and C\_4 = Bare land, UA = User Accuracy, PA = Producer Accuracy, OA = Overall Accuracy, Kc = Kappa Coefficient).

## Data availability

The open source satellite data was collected from USGS server (<https://earthexplorer.usgs.gov/>) and Google Earth Pro 7.3.6.10201 (Google LLC, <https://earth.google.com>). The reclassification codes are supplied in Table S 5. The classified land cover maps will be made available upon reasonable request from the corresponding author [Md. Sharafat Chowdhury, email: sharafat.44@geography-juniv.edu.bd; sharafat.geography.juniv@gmail.com].

Received: 25 October 2024; Accepted: 25 August 2025

Published online: 06 January 2026

## References

- Winkler, K., Fuchs, R., Rounsevell, M. & Herold, M. Global land use changes are four times greater than previously estimated. *Nat. Commun.* **12**, 2501. <https://doi.org/10.1038/s41467-021-22702-2> (2021).
- Zhu, Z., Wang, S. & Woodcock, C. E. Improvement and expansion of the Fmask algorithm: cloud, cloud shadow, and snow detection for Landsats 4–7, 8, and Sentinel 2 images. *Remote Sens. Environ.* **159**, 269–277. <https://doi.org/10.1016/j.rse.2014.12.014> (2020).
- Li, W., Fu, H., Yu, L. & Gong, P. Integrating multi-seasonal Sentinel-2 imagery for land cover classification using a dual-branch convolutional neural network. *Remote Sens. Environ.* **252**, 112150. <https://doi.org/10.1016/j.rse.2020.112150> (2021).
- Findell, K. L. et al. The impact of anthropogenic land use and land cover change on regional climate extremes. *Nat. Commun.* **8**, 989. <https://doi.org/10.1038/s41467-017-01038-w> (2017).
- Kumar, S. et al. Changes in land use enhance the sensitivity of tropical ecosystems to fire-climate extremes. *Sci. Rep.* **12**, 964. <https://doi.org/10.1038/s41598-022-05130-0> (2022b).
- Dewan, A. M. & Yamaguchi, Y. Land use and land cover change in greater dhaka, bangladesh: using remote sensing to promote sustainable urbanization. *Appl. Geogr.* **29**, 390–401. <https://doi.org/10.1016/j.apgeog.2008.12.005> (2009a).
- Alemayehu, F. et al. The impacts of watershed management on land use and land cover dynamics in Eastern Tigray (Ethiopia). *Resour. Conserv. Recycl.* **53**, 192–198. <https://doi.org/10.1016/j.resconrec.2008.11.007> (2009).
- Rajaei, F. et al. Application of integrated watershed management measures to minimize the land use change impacts. *Water* **13**, 2039. <https://doi.org/10.3390/w13152039> (2021).
- Hoque, M. Z., Islam, I., Ahmed, M., Hasan, S. S. & Prodhan, F. A. Spatio-temporal changes of land use land cover and ecosystem service values in coastal Bangladesh. *Egypt. J. Remote Sens. Space Sci.* **25**, 173–180. <https://doi.org/10.1016/j.ejrs.2022.01.008> (2022).
- Kumar, A., Diksha, Pandey, A. C. & Khan, M. L. Urban risk and resilience to climate change and natural hazards: a perspective from million-plus cities on the Indian Subcontinent. *Techniques Disaster Risk Manage. Mitigation.* 33–46. <https://doi.org/10.1002/9781119359203.ch3> (2020).
- Rojas, C., Pino, J., Basnou, C. & Vivanco, M. Assessing land-use and-cover changes in relation to geographic factors and urban planning in the metropolitan area of Concepción (Chile). Implications for biodiversity conservation. *Appl. Geogr.* **39**, 93–103. <https://doi.org/10.1016/j.apgeog.2012.12.007> (2013).
- He, C., Liu, Z., Tian, J. & Ma, Q. Urban expansion dynamics and natural habitat loss in china: A multiscale landscape perspective. *Glob Change Biol.* **20**, 2886–2902. <https://doi.org/10.1111/gcb.12553> (2014).
- Zhai, T. et al. Assessing ecological risks caused by human activities in rapid urbanization coastal areas: towards an integrated approach to determining key areas of terrestrial-oceanic ecosystems preservation and restoration. *Sci. Total Environ.* **708**, 135153. <https://doi.org/10.1016/j.scitotenv.2019.135153> (2020).
- Xie, H., Zhang, Y., Zeng, X. & He, Y. Sustainable land use and management research: A scientometric review. *Landsc. Ecol.* **35**, 2381–2411. <https://doi.org/10.1007/s10980-020-01002-y> (2020).

15. Hassan, M. M. & Southworth, J. Analyzing land cover change and urban growth trajectories of the mega-urban region of Dhaka using remotely sensed data and an ensemble classifier. *Sustainability* **10**, 10. <https://doi.org/10.3390/su10010010> (2017).
16. Nitze, I., Barrett, B. & Cawkwell, F. Temporal optimisation of image acquisition for land cover classification with random forest and MODIS time-series. *Int. J. Appl. Earth Obs Geoinf.* **34**, 136–146. <https://doi.org/10.1016/j.jag.2014.08.001> (2015).
17. Karila, K., Matikainen, L., Litkey, P., Hyypä, J. & Puttonen, E. The effect of seasonal variation on automated land cover mapping from multispectral airborne laser scanning data. *Int. J. Remote Sens.* **40**, 3289–3307. <https://doi.org/10.1080/01431161.2018.1528023> (2019).
18. Sresto, M. A., Siddika, S., Fattah, M. A., Morshed, S. R. & Morshed, M. M. A GIS and remote sensing approach for measuring summer-winter variation of land use and land cover indices and surface temperature in Dhaka district. *Bangladesh Heliyon*. **8**, e10309. <https://doi.org/10.1016/j.heliyon.2022.e10309> (2022).
19. Nur, S. M. S. & Mitra, C. Urban growth and Multi-seasonal land cover classification of dhaka, bangladesh: an approach using Google Earth engine. In *Urban Transformational Landscapes in the City-Hinterlands of Asia. Advances in 21st Century Human Settlements* (eds Mookherjee, D. et al.) 199–219 (Springer, 2023).
20. Reed, B. C. et al. Measuring phenological variability from satellite imagery. *J. Veg. Sci.* **5**, 703–714. <https://doi.org/10.2307/3235884> (1994).
21. Silveira, E. M. et al. Reducing the effects of vegetation phenology on change detection in tropical seasonal biomes. *GIScience Remote Sens.* **56** (5), 699–717. <https://doi.org/10.1080/15481603.2018.1550245> (2019).
22. Wang, X. et al. Slower changes in vegetation phenology than precipitation seasonality in the dry tropics. *Glob. Change Biol.* **30** (1), 123–136. <https://doi.org/10.1111/gcb.17134> (2024).
23. Ishan, R. & Intezar, T. An Analysis on Chronological Conversion of Urban Wetlands of Dhaka Metropolitan Area from 1990 to (2019). (2018).
24. Imran, H. M. et al. Impact of land cover changes on land surface temperature and human thermal comfort in Dhaka City of Bangladesh. *Earth Syst. Environ.* **5**, 667–693. <https://doi.org/10.1007/s41748-021-00243-4> (2021).
25. Kafy, A. A. et al. Modeling the relationship between land use/land cover and land surface temperature in dhaka, Bangladesh using CA-ANN algorithm. *Environ. Chall.* **4**, 100190. <https://doi.org/10.1016/j.envc.2021.100190> (2021a).
26. Hossein, M. K. et al. Prediction of land use and land cover changes (LULC) and urban growth analysis in Dhaka metropolitan area (DMA) using CA-Markov model and Geospatial techniques. *Arab. J. Geosci.* **16**, 468. <https://doi.org/10.1007/s12517-023-11570-3> (2023).
27. Nasiri, V. et al. Land use and land cover mapping using Sentinel-2, Landsat-8 satellite images, and Google Earth engine: A comparison of two composition methods. *Remote Sens.* **14**, 1977. <https://doi.org/10.3390/rs14091977> (2022).
28. Zhou, T., Zhao, M., Sun, C. & Pan, J. Exploring the impact of seasonality on urban land-cover mapping using multi-season sentinel-1a and gf-1 Wfv images in a subtropical monsoon-climate region. *ISPRS Int. J. Geo-Inf.* **7**, 3. <https://doi.org/10.3390/ijgi7010003> (2017).
29. Yimer, A. K., Haile, A. T., Hatiye, S. D. & Azeref, A. G. Seasonal effect on the accuracy of land use/land cover classification in the bilate Sub-basin, Abaya-Chamo basin, rift Valley lakes basin of Ethiopia. *Ethiop. J. Water Sci. Technol.* **3**, 23–50. <https://doi.org/10.59122/134C842> (2020).
30. Liu, J., Heiskanen, J., Aynekulu, E., Maeda, E. E. & Pellikka, P. K. Land cover characterization in West Sudanian savannas using seasonal features from annual Landsat time series. *Remote Sens.* **8**, 365. <https://doi.org/10.3390/rs8050365> (2016).
31. Lopes, M. et al. Improving the accuracy of land cover classification in cloud persistent areas using optical and radar satellite image time series. *Methods Ecol. Evol.* **11**, 532–541. <https://doi.org/10.1111/2041-210X.13359> (2020).
32. Zhu, L., La, Y., Shi, R. & Peng, S. Land Cover Spurious Change Detection Using a geo-eco Zoning Rule Base. In *IGARSS 2019–2019 IEEE International Geoscience and Remote Sensing Symposium* 6507–6510IEEE, (2019).
33. Liu, J., Heiskanen, J., Aynekulu, E. & Pellikka, P. K. E. Seasonal variation of land cover classification accuracy of Landsat 8 images in Burkina Faso. *Int. Arch. Photogramm Remote Sens. Spat. Inf. Sci.* **40**, 455–460. <https://doi.org/10.5194/isprsarchives-XL-7-W3-455-2015> (2015).
34. Kafy, A. A. et al. Assessing and predicting land use/land cover, land surface temperature and urban thermal field variance index using Landsat imagery for Dhaka metropolitan area. *Environ. Chall.* **4**, 100192. <https://doi.org/10.1016/j.envc.2021.100192> (2021b).
35. Ahmed, B., Kamruzzaman, M. D., Zhu, X., Rahman, M. S. & Choi, K. Simulating land cover changes and their impacts on land surface temperature in dhaka, Bangladesh. *Remote Sens.* **5**, 5969–5998. <https://doi.org/10.3390/rs5115969> (2013).
36. Morshed, N., Yorke, C. & Zhang, Q. Urban expansion pattern and land use dynamics in dhaka, 1989–2014. *Prof. Geogr.* **69**, 396–411. <https://doi.org/10.1080/00330124.2016.1268058> (2017).
37. Sarmah, T. & Das, S. Urban flood mitigation planning for guwahati: A case of Bharalu basin. *J. Environ. Manag.* **206**, 1155–1165. <https://doi.org/10.1016/j.jenvman.2017.10.079> (2018).
38. Moniruzzaman, M. et al. Decadal urban land use/land cover changes and its impact on surface runoff potential for the Dhaka City and surroundings using remote sensing. *Remote Sens.* **13**, 83. <https://doi.org/10.3390/rs13010083> (2020).
39. Dewan, A. M., Yamaguchi, Y. & Rahman, M. Z. Dynamics of land use/cover changes and the analysis of landscape fragmentation in Dhaka metropolitan. *Bangladesh Geojournal.* **77**, 315–330. <https://doi.org/10.1007/s10708-010-9399-x> (2012).
40. Nawar, N., Sorker, R., Chowdhury, F. J. & Rahman, M. M. Present status and historical changes of urban green space in Dhaka city, bangladesh: A remote sensing driven approach. *Environ. Challenges.* **6**, 100425. <https://doi.org/10.1016/j.envc.2021.100425> (2022).
41. Ahmed, B. & Ahmed, R. Modeling urban land cover growth dynamics using multi Temporal satellite images: A case study of dhaka, Bangladesh. *ISPRS Int. J. Geo-Inf.* **1**, 3–31. <https://doi.org/10.3390/ijgi1010003> (2012).
42. Roy, S. K. et al. Dynamic assessment and prediction of land use alterations influence on ecosystem service value: A pathway to environmental sustainability. *Environ. Sustain. Indic.* **21**, 100319. <https://doi.org/10.1016/j.indic.2023.100319> (2024).
43. Shahid, S. et al. Climate variability and changes in the major cities of bangladesh: observations, possible impacts and adaptation. *Reg. Environ. Change.* **16**, 459–471. <https://doi.org/10.1007/s10113-015-0757-6> (2016).
44. Hossain, M. J., Mahmud, M. M. & Islam, S. T. Monitoring Spatiotemporal changes of urban surface water based on satellite imagery and Google Earth engine platform in Dhaka City from 1990 to 2021. *Bull. Natl. Res. Cent.* **47**, 150. <https://doi.org/10.1186/s42269-023-01127-5> (2023).
45. Ahmed, B. Urban land cover change detection analysis and modeling spatio-temporal growth dynamics using remote sensing and GIS techniques: A case study of Dhaka, Bangladesh. Master's thesis, Universidade NOVA de Lisboa (Portugal) (2011).
46. Dewan, A. M. & Yamaguchi, Y. Using remote sensing and GIS to detect and monitor land use and land cover change in Dhaka metropolitan of Bangladesh during 1960–2005. *Environ. Monit. Assess.* **150**, 237–249. <https://doi.org/10.1007/s10661-008-0226-5> (2009b).
47. Khan, S., Hossain, S. & Uddin, M. S. An Advanced Surveillance System to Monitor Wetland Changes—A Case Study on Dhaka City. In *10th Global Engineering, Science and Technology Conference, BIAM Foundation, Dhaka, Bangladesh* 1–11 (2015).
48. Sultana, M. S., Islam, G. M. T. & Zahidul, I. Pre- and post-urban wetland area in Dhaka city, bangladesh: a remote sensing and GIS analysis. *J. Water Resour. Prot.* **1**, 414–421. <https://doi.org/10.4236/jwarp.2009.16050> (2009).
49. Islam, M. S., Shahabuddin, A. K. M., Kamal, M. M. & Ahmed, R. Wetlands of Dhaka city: its past and present scenario. *J. Life Earth Sci.* **7**, 83–90. <https://doi.org/10.3329/jles.v7i0.20126> (2010).

50. Mahmud, M. S., Masrur, A., Ishtiaque, A., Haider, F. & Habiba, U. Remote sensing & GIS based spatio-temporal change analysis of wetland in Dhaka city, Bangladesh. *J. Water Resour. Prot.* **3**, 781. <https://doi.org/10.4236/jwarp.2011.311088> (2011).
51. Sultana, J. N. & Hafiz, R. The Circular Waterway: Saving Rivers of Dhaka by Enhancing Recreation and Place-Making Along Specific Routes. *J. Bangladesh Inst. Planners* 9363 (2013). Link: (2075). <https://www.bip.org.bd/admin/uploads/bip-publication/publication-11/paper/20141016155226.pdf>
52. Alam, M. J. & Ahmad, M. M. Analysing the lacunae in planning and implementation: Spatial development of Dhaka City and its impacts upon the built environment. *Int. J. Urban Sustain. Dev.* **2**, 85–106. <https://doi.org/10.1080/19463138.2010.512809> (2010).
53. Huq, H. Study on land-use and land cover change of Dhaka eastern region and its impact on water cycle. (2017).
54. Pia, N. A. Rethinking residential neighborhood in dhaka, bangladesh: Jane jacobs's urban design principles for improving livability. In *Urban and Transit Planning. Advances in Science, Technology & Innovation* (eds Alberti, F. et al.) 177–191 (Springer, 2022).
55. Parvin, N., Khatun, A., Quais, M. K. & Nasim, M. Cropping pattern, intensity and diversity in Dhaka region. *Bangladesh Rice J.* **21**, 123–141 (2018).
56. Kafy, A. A. et al. Cellular automata approach in dynamic modelling of land cover changes using RapidEye images in dhaka, Bangladesh. *Environ. Chall.* **4**, 100084. <https://doi.org/10.1016/j.envc.2021.100084> (2021c).
57. Byomkesh, T., Nakagoshi, N. & Dewan, A. M. Urbanization and green space dynamics in greater dhaka, Bangladesh. *Landsc. Ecol. Eng.* **8**, 45–58. <https://doi.org/10.1007/s11355-010-0147-7> (2012).
58. Siddiqua, F. Z. Dhaka needs more trees, but... The Daily Star (2017). <https://www.thedailystar.net/star-weekend/dhaka-needs-more-trees-1414189>.
59. Jaman, M., Jahan, I., Jamil, M. & Hossain, M. Structure and composition of plant across different urban land vegetation in Dhaka South city, Bangladesh. *J. Agric. Ecol. Res. Int.* **13**, 1–14. <https://doi.org/10.9734/AERI/2017/38562> (2017).
60. Sultana, R. Greening the slums: Urban green infrastructure in Dhaka, Bangladesh. Master's thesis, University of Wollongong (2020).
61. Subrina, S. & Chowdhury, F. K. Urban dynamics: an undervalued issue for water logging disaster risk management in case of Dhaka city, Bangladesh. *Procedia Eng.* **212**, 801–808. <https://doi.org/10.1016/j.proeng.2018.01.103> (2018).
62. Mia, B., Bhattacharya, R. & Woobaidullah, A. S. M. Correlation and monitoring of land surface temperature, urban heat Island with land use-land cover of Dhaka City using satellite imageries. *Int. J. Res. Geogr.* **3**, 10–20 (2017).
63. Heaviside, C., Macintyre, H. & Vardoulakis, S. The urban heat island: implications for health in a changing environment. *Curr. Envir Health Rpt.* **4**, 296–305. <https://doi.org/10.1007/s40572-017-0150-3> (2017).
64. Ahmed, F., Moors, E., Khan, M. S. A., Warner, J. & Van Scheltinga, C. T. Tipping points in adaptation to urban flooding under climate change and urban growth: the case of the Dhaka megacity. *Land. Use Policy.* **79**, 496–506. <https://doi.org/10.1016/j.landusepol.2018.05.051> (2018).
65. Sakib, M. S. et al. I. A. Impact of urbanization on pluvial flooding: insights from a fast growing megacity, Dhaka. *Water* **15**, 3834. <https://doi.org/10.3390/w15213834> (2023).
66. Huong, H. T. L. & Pathirana, A. Urbanization and climate change impacts on future urban flooding in can tho city, Vietnam. *Hydrol. Earth Syst. Sci.* **17**, 379–394. <https://doi.org/10.5194/hess-17-379-2013> (2013).
67. Ma, B., Wu, Z., Wang, H. & Guo, Y. Study on the classification of urban waterlogging rainstorms and rainfall thresholds in cities lacking actual data. *Water* **12**, 3328. <https://doi.org/10.3390/w12123328> (2020).
68. Cohen, B. Urbanization in developing countries: current trends, future projections, and key challenges for sustainability. *Technol. Soc.* **28**, 63–80. <https://doi.org/10.1016/j.techsoc.2005.10.005> (2006).
69. Roy, M. Planning for sustainable urbanisation in fast growing cities: mitigation and adaptation issues addressed in dhaka, Bangladesh. *Habitat Int.* **33**, 276–286. <https://doi.org/10.1016/j.habitatint.2008.10.022> (2009).
70. Morabito, M. et al. The impact of built-up surfaces on land surface temperatures in Italian urban areas. *Sci. Total Environ.* **551**, 317–326. <https://doi.org/10.1016/j.scitotenv.2016.02.029> (2016).
71. Gunawardena, K. R., Wells, M. J. & Kershaw, T. Utilising green and Bluespace to mitigate urban heat Island intensity. *Sci. Total Environ.* **584**, 1040–1055. <https://doi.org/10.1016/j.scitotenv.2017.01.158> (2017).
72. Mohajerani, A., Bakaric, J. & Jeffrey-Bailey, T. The urban heat Island effect, its causes, and mitigation, with reference to the thermal properties of asphalt concrete. *J. Environ. Manage.* **197**, 522–538. <https://doi.org/10.1016/j.jenvman.2017.03.095> (2017).
73. Varma, K., Srivastava, V., Singhal, A. & Jha, P. K. Urban and environmental hazards. In *Recent Technologies for Disaster Management and Risk Reduction* (eds Rai, P. K. et al.) 761–781 (Springer, 2021). [https://doi.org/10.1007/978-3-030-76116-5\\_19](https://doi.org/10.1007/978-3-030-76116-5_19).
74. Bibi, S. T. & Kara, G. K. Evaluation of climate change, urbanization, and low-impact development practices on urban flooding. *Heliyon* **9**, e12955. <https://doi.org/10.1016/j.heliyon.2023.e12955> (2023).
75. Wu, J. et al. Assessing urban pluvial waterlogging resilience based on sewer congestion risk and climate change impacts. *J. Hydrol.* **626**, 130230. <https://doi.org/10.1016/j.jhydrol.2023.130230> (2023).
76. Hossain, M. S. & Rahman, M. Assessment of Land Use/Land Cover (LULC) Changes and Urban Growth Dynamics Using Remote Sensing in Dhaka City, Bangladesh. In *ICSBE 2020: Proceedings of the 11th International Conference on Sustainable Built Environment* 611–621 (Springer Singapore, 2022). [https://doi.org/10.1007/978-981-16-4412-2\\_48](https://doi.org/10.1007/978-981-16-4412-2_48)
77. Al Jaber, S., Ghosh, A. K. & Mahmud, M. S. Using time series of satellite images to detect vegetation cover change in Dhaka City. *J. Geogr. Inf. Syst.* **6**, 653. <https://doi.org/10.4236/jgis.2014.66054> (2014).
78. Rahman, M. M. & Szabó, G. Impact of land use and land cover changes on urban ecosystem service value in Dhaka. *Bangladesh Land.* **10**, 793. <https://doi.org/10.3390/land10080793> (2021).
79. Karim, M. A. Urban expansion in dhaka and its heat island effect. *The Business Standard* Accessed 5 January 2024. (2021). Available at: <https://www.tbsnews.net/thoughts/urban-expansion-dhaka-and-its-heat-island-effect-292240>
80. RAJUK. *Dhaka Structure Plan, 1995–2015* (DMDP, 1995).
81. RAJUK. *Dhaka structure plan, 2016–2035*. DMDP. (2015). Retrieved from [https://rajuk.portal.gov.bd/sites/default/files/files/rajuk.portal.gov.bd/page/0a05e9d0\\_03f7\\_48e4\\_bfd5\\_cad5fbcd5e23/2021-06-22-08-35-c8b98a96d0cad8d87fa1c61f56966bb.pdf](https://rajuk.portal.gov.bd/sites/default/files/files/rajuk.portal.gov.bd/page/0a05e9d0_03f7_48e4_bfd5_cad5fbcd5e23/2021-06-22-08-35-c8b98a96d0cad8d87fa1c61f56966bb.pdf)
82. Das, J., Mandal, T., Rahman, A. T. M. & Saha, P. Spatio-temporal characterization of rainfall in bangladesh: an innovative trend and discrete wavelet transformation approaches. *Theoret. Appl. Climatol.* **143** (3), 1557–1579. <https://doi.org/10.1007/s00704-020-03508-6> (2021).
83. Khan, M. H. R. et al. Detection of changes and trends in Climatic variables in Bangladesh during 1988–2017. *Heliyon* **5** (3), e01268. <https://doi.org/10.1016/j.heliyon.2019.e01268> (2019).
84. Moravec, D., Komárek, J., López-Cuervo Medina, S. & Molina, I. Effect of atmospheric corrections on NDVI: intercomparability of Landsat 8, Sentinel-2, and UAV sensors. *Remote Sens.* **13** (18), 3550. <https://doi.org/10.3390/rs13183550> (2021).
85. Zhang, Z., He, G. & Wang, X. A practical DOS model-based atmospheric correction algorithm. *Int. J. Remote Sens.* **31** (11), 2837–2852. <https://doi.org/10.1080/01431160903124682> (2010).
86. Nazeer, M., Nichol, J. E. & Yung, Y. K. Evaluation of atmospheric correction models and Landsat surface reflectance product in an urban coastal environment. *Int. J. Remote Sens.* **35** (16), 6271–6291. <https://doi.org/10.1080/01431161.2014.951742> (2014).
87. Dewi, E. K. & Trisakti, B. Comparing atmospheric correction methods for Landsat OLI data. *Int. J. Remote Sens. Earth Sci. (IJReSES)*. **13** (2), 105–120. <https://doi.org/10.30536/j.ijreses.2016.v13.a2472> (2017).
88. Lhissou, R., Harti, E., Maimouni, A., Adiri, Z. & S. and Assessment of the image-based atmospheric correction of multispectral satellite images for geological mapping in arid and semi-arid regions. *Remote Sens. Applications: Soc. Environ.* **20**, 100420. <https://doi.org/10.1016/j.rsase.2020.100420> (2020).

89. Shahvaran, A. R., Kheyrollah Pour, H. & Van Cappellen, P. Comparative evaluation of Semi-Empirical approaches to retrieve Satellite-Derived Chlorophyll-a concentrations from nearshore and offshore waters of a large lake (Lake Ontario). *Remote Sens.* **16** (9), 1595. <https://doi.org/10.3390/rs16091595> (2024).
90. Rumora, L., Miler, M. & Medak, D. Contemporary comparative assessment of atmospheric correction influence on radiometric indices between Sentinel-2A and Landsat 8 imagery. *Geocarto Int.* **36** (1), 13–27 (2021).
91. Karimi, B., Hashemi, S. H. & Aghighi, H. Application of Landsat-8 and Sentinel-2 for retrieval of chlorophyll-a in a shallow freshwater lake. *Adv. Space Res.* **74** (1), 117–129. <https://doi.org/10.1016/j.asr.2024.03.056> (2024).
92. Leroux, L., Congedo, L., Bellón, B., Gaetano, R. & Bégué, A. Land cover mapping using Sentinel-2 images and the semi-automatic classification plugin: A Northern Burkina Faso case study. *QGIS Appl. Agric. For.* **2**, 119–151. <https://doi.org/10.1002/9781119457107.ch4> (2018).
93. Issiako, D., Arouna, O., Soufianou, K., Imorou, I. T. & Tente, B. Prospective mapping of land cover and land use in the classified forest of the upper Alibori based on satellite imagery. *Geoplanning* **8**, 115–126. <https://doi.org/10.14710/geoplanning.8.2.115-126> (2021).
94. Bui, D. H. & Mucsi, L. From land cover map to land use map: A combined pixel-based and object-based approach using multi-temporal Landsat data, a random forest classifier, and decision rules. *Remote Sens.* **13**, 1700. <https://doi.org/10.3390/rs13091700> (2021).
95. Purwanto, A. D., Wikantika, K., Deliar, A. & Darmawan, S. Decision tree and random forest classification algorithms for Mangrove forest mapping in Sembilang National park, Indonesia. *Remote Sens.* **15**, 16. <https://doi.org/10.3390/rs15010016> (2022).
96. Foody, G. M. Explaining the unsuitability of the kappa coefficient in the assessment and comparison of the accuracy of thematic maps obtained by image classification. *Remote Sens. Environ.* **239**, 111630. <https://doi.org/10.1016/j.rse.2019.111630> (2020).
97. Phan, D. C. et al. First comprehensive quantification of annual land use/cover from 1990 to 2020 across Mainland Vietnam. *Sci. Rep.* **11**, 9979. <https://doi.org/10.1038/s41598-021-89034-5> (2021).
98. Osgouei, E. P., Sertel, E. & Kabadayı, M. E. Integrated usage of historical Geospatial data and modern satellite images reveal long-term land use/cover changes in bursa/turkey, 1858–2020. *Sci. Rep.* **12**, 9077. <https://doi.org/10.1038/s41598-022-11396-1> (2022).
99. Mugabowindekwe, M. et al. Trees on smallholder farms and forest restoration are critical for Rwanda to achieve net zero emissions. *Commun. Earth Environ.* **5**, 113. <https://doi.org/10.1038/s43247-024-01278-x> (2024).
100. Kammerer, M., Iverson, A. L., Li, K. & Goslee, S. C. Not just crop or forest: an integrated land cover map for agricultural and natural areas. *Sci. Data.* **11**, 137. <https://doi.org/10.1038/s41597-024-02979-w> (2024).
101. Kerner, H. et al. How accurate are existing land cover maps for agriculture in Sub-Saharan africa?? *Sci. Data.* **11**, 486. <https://doi.org/10.1038/s41597-024-03306-z> (2024).
102. Zhao, Z. et al. Comparison of three machine learning algorithms using Google Earth engine for land use land cover classification. *Rangel. Ecol. Manag.* **92**, 129–137. <https://doi.org/10.1016/j.rama.2023.10.007> (2024).
103. Asadi, B. & Shamsoddini, A. Crop mapping through a hybrid machine learning and deep learning method. *Remote Sens. Appl. Soc. Environ.* **33**, 101090. <https://doi.org/10.1016/j.rsase.2023.101090> (2024).
104. Eker, R., Bühler, Y., Schlögl, S., Stoffel, A. & Aydın, A. Monitoring of snow cover ablation using very high Spatial resolution remote sensing datasets. *Remote Sens.* **11**, 699. <https://doi.org/10.3390/rs11060699> (2019).
105. Li, Z. et al. Accuracy assessment of land cover products in China from 2000 to 2020. *Sci. Rep.* **13**, 12936. <https://doi.org/10.1038/s41598-023-39963-0> (2023).

## Acknowledgements

I would like to extend my gratitude to the anonymous reviewers for their valuable comments, which have helped to improve the quality of the manuscript.

## Author contributions

Md. Sharafat Chowdhury: Conceptualization, Data curation, Formal analysis, Investigation, Methodology, Project administration, Software, Validation, Visualization, Writing – original draft, Writing – review & editing.

## Declarations

## Competing interests

The authors declare no competing interests.

## Additional information

**Supplementary Information** The online version contains supplementary material available at <https://doi.org/10.1038/s41598-025-17478-0>.

**Correspondence** and requests for materials should be addressed to M.S.C.

**Reprints and permissions information** is available at [www.nature.com/reprints](http://www.nature.com/reprints).

**Publisher's note** Springer Nature remains neutral with regard to jurisdictional claims in published maps and institutional affiliations.

**Open Access** This article is licensed under a Creative Commons Attribution-NonCommercial-NoDerivatives 4.0 International License, which permits any non-commercial use, sharing, distribution and reproduction in any medium or format, as long as you give appropriate credit to the original author(s) and the source, provide a link to the Creative Commons licence, and indicate if you modified the licensed material. You do not have permission under this licence to share adapted material derived from this article or parts of it. The images or other third party material in this article are included in the article's Creative Commons licence, unless indicated otherwise in a credit line to the material. If material is not included in the article's Creative Commons licence and your intended use is not permitted by statutory regulation or exceeds the permitted use, you will need to obtain permission directly from the copyright holder. To view a copy of this licence, visit <http://creativecommons.org/licenses/by-nc-nd/4.0/>.

© The Author(s) 2026